N72-30388

CASE FILE COPY

ELECTROMAGNETIC DAMPER SYSTEM FOR GROUND WIND LOAD STUDIES

FINAL REPORT

Contract NAS8-26774

May 1972

CR-123799

Lockheed

HUNTSVILLE RESEARCH & ENGINEERING CENTER

LOCKHEED MISSILES & SPACE COMPANY, INC.
A SUBSIDIARY OF LOCKHEED AIRCRAFT CORPORATION

HUNTSVILLE, ALABAMA

HREC-6674-1
LMSC-HREC D225690

LOCKHEED MISSILES & SPACE COMPANY
HUNTSVILLE RESEARCH & ENGINEERING CENTER
HUNTSVILLE RESEARCH PARK
4800 BRADFORD DRIVE, HUNTSVILLE, ALABAMA

ELECTROMAGNETIC DAMPER SYSTEM FOR GROUND WIND LOAD STUDIES

FINAL REPORT

Contract NAS8-26774

May 1972

Prepared for National Aeronautics and Space Administration
Marshall Space Flight Center, Alabama 35812

by

L. P. Scott

APPROVED:

W. L. Swanson, Supervisor
Acoustics Section

Donald McDonald, Manager
Structures & Mechanics Dept.

J. S. Farrior
Resident Director

CONTENTS

Section 1
INTRODUCTION AND SUMMARY

Wind tunnel tests of aeroelastic scale models provide a means of investigating the aerodynamic forces (and projected responses) resulting from wind flow past the full-scale vehicle in the prelaunch condition. For determining the unsteady dynamic loads induced by these ground wind environments, a 5.5% Saturn IB model was constructed by NASA-MSFC and later modified to simulate the Saturn IB/Skylab launch vehicle. Lockheed-Huntsville provided assistance in designing and evaluating these modifications. Under an earlier contract effort (NAS8-15483) Lockheed-Huntsville developed a model damper system for ground winds models.

The damper system has been continually refined for use with both Saturn IB and V aeroelastic models. Accurate remote control and adjustment of test model structural damping levels is accomplished by this system. The servo-feedback controlled electromagnetic shaker acts as a simulator of linear structural damping forces during the wind tunnel tests.

The primary task of this work effort was to design, fabricate, and adapt the model damper system to the 5.5% aeroelastic model of the Saturn IB/Skylab launch vehicle. In addition, the damper was dynamically calibrated over the desired range of additive damping for each of the model conditions prior to wind tunnel testing. And, finally, the system was transported to the test site at Langley Field, Virginia where assistance in setup, instrumentation, and test procedures was provided. When the tests were completed, recordings of the model response signals for certain test points were submitted to Power Spectral Density Analyses at Lockheed-Huntsville.

Individual tasks are discussed chronologically in the following sections. This final report summarizes the entire scope of the contract work effort. Detailed information may be found in the following document and drawing:

1. Scott, L. P., "Saturn IB/Skylab Model Damper Installation and Operation Manual," LMSC-HREC D225270, Lockheed Missiles & Space Company, Huntsville, Ala., August 6, 1971.

   (This interim document describes the installation, checkout, and calibration of the damper system prior to wind tunnel testing.)

2. Lockheed Drawing No. R 72107, Revision A – Damper System Assembly, dated 3-2-71.

   (This drawing details the mechanical components of the Saturn IB/Skylab damper and presents an assembly of the system showing model interface details.)

Section 2
MODEL DAMPER SYSTEM DESIGN AND FABRICATION

The design and construction of the model damper system is divided into three subsections: (a) Mechanical Equipment, (b) Electronic Control and Instrumentation, and (c) Model Design Changes for Damper Installation.

2.1 MECHANICAL EQUIPMENT

The previously noted Lockheed drawing presents the major mechanical components of the damper system which utilizes two Ling V-50A, 50-pound shakers fitted atop a support post with their force axes at 90°. The support post for use with the Saturn IB/Skylab model was fabricated with a small flexure at its base which yields a low first natural frequency of the post/shaker assembly (about 1.0 Hz), and thus isolates the system from participation or effect in the model dynamic response. Figure 2-1 shows the model-damper configuration and identifies the interface points.

The damper/shaker package is attached to the model by double-pivoted flexures which transmit the additive damping forces to the model structure. These flexures are fitted with load cells for the monitoring and/or recording of damping force levels. Velocity sensors are positioned on the interior walls of the model in the area of the damper and act as the generators of the feedback control velocity signal.

The damper post is fitted with an adjustable torsion bar which provides a return-to-center spring force in the radial direction and allows exact alignment to be made. The damper position in the vertical direction is adjusted by spacers (shims) beneath the supporting angle bracket on the lower shaker. An adjustable bracket between the shakers provides for relative alignment between the flexure axes. Lead counterweights are fitted to the face of each shaker for proper positioning of each shaker's c.g. exactly over the center of the support post. This eliminates the unbalance of the assembly and allows longer flexures (and thus better directional isolation between the two shaker axes).

2.2 ELECTRONIC CONTROL AND INSTRUMENTATION

The output of each velocity sensor is the input to the damper control circuit. Duplicate channels individually control each shaker. A circuit diagram of one of the control channels with its calibration circuit is shown in Fig. 2-2. After it passes through the input (buffer) amplifier this control signal is input to an adjustable circuit which includes a 100KΩ variable damping potentiometer. The calibration of this pot and its variable setting controls the adjustment of the additive damping forces fed back to the model. After summing with an oscillator signal (used for the calibration excitation) the combined signal passes to the power amplifier (Ling TP-850), and thence through a long power cable to the shakers. The control loop is closed by the oscillating model which generates the velocity feedback signal.

The electronic components associated with each control channel are incorporated into a circuit board mounted in the damper system control console. Numerous auxiliary amplifier input and output terminals are available on the face of the console for patching into the desired circuits. The power amplifiers are positioned in the base of the console and four charge amplifiers are also present. Two of these are for use with the piezoelectric load cells and the other two are available for use with model-associated accelerometers. The use of these type sensors/amplifiers and the micro-dot cables eliminates the effect of long cable lengths and affords accurate measurement and control from a remote location.

2.3 MODEL DESIGN CHANGES FOR DAMPER INSTALLATION

Because of the requirement of high force levels at the shaker (for high additive damping levels) the shaker package should be positioned as high as

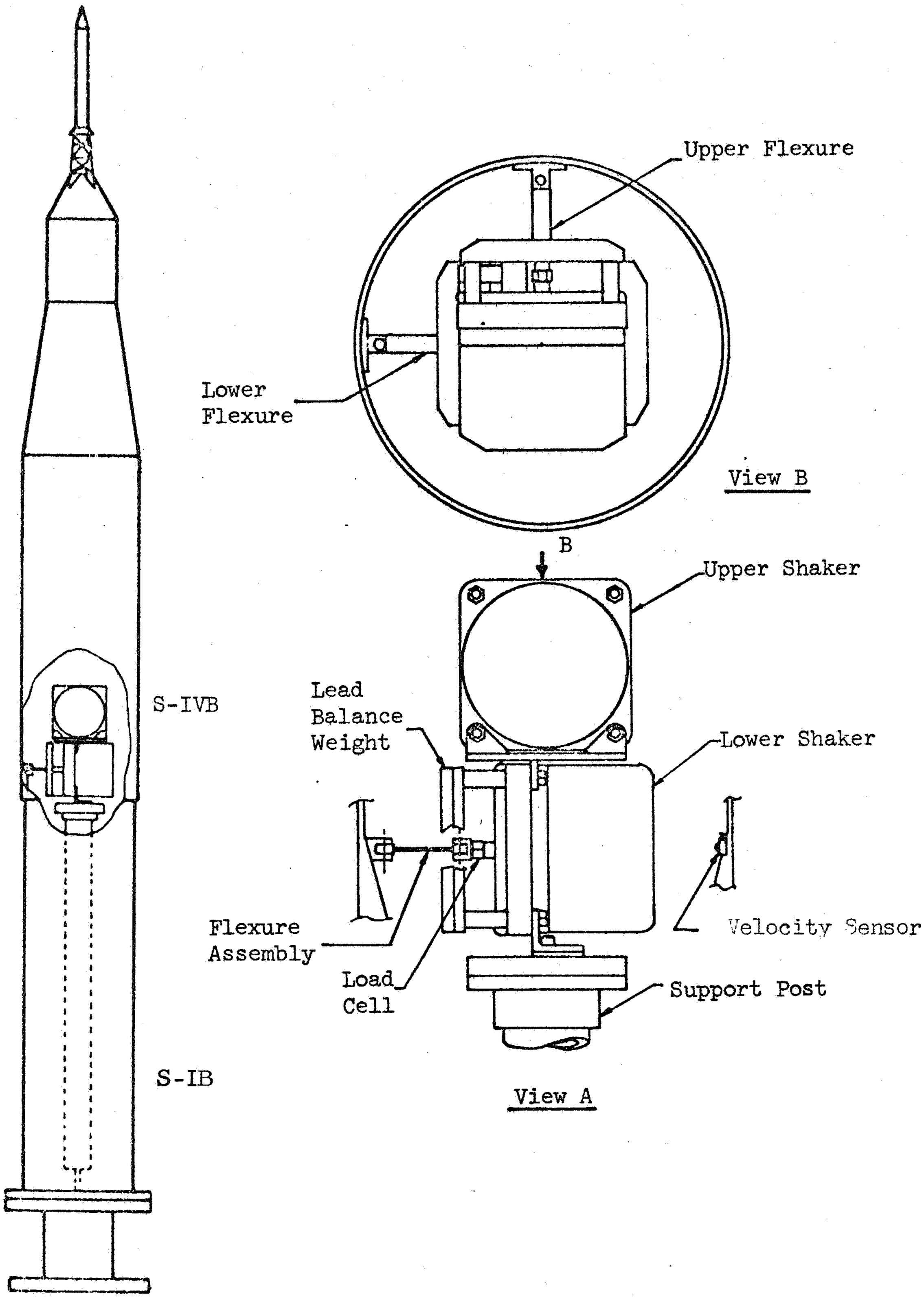

Fig. 2-1 - Model-Damper Configuration and Interface

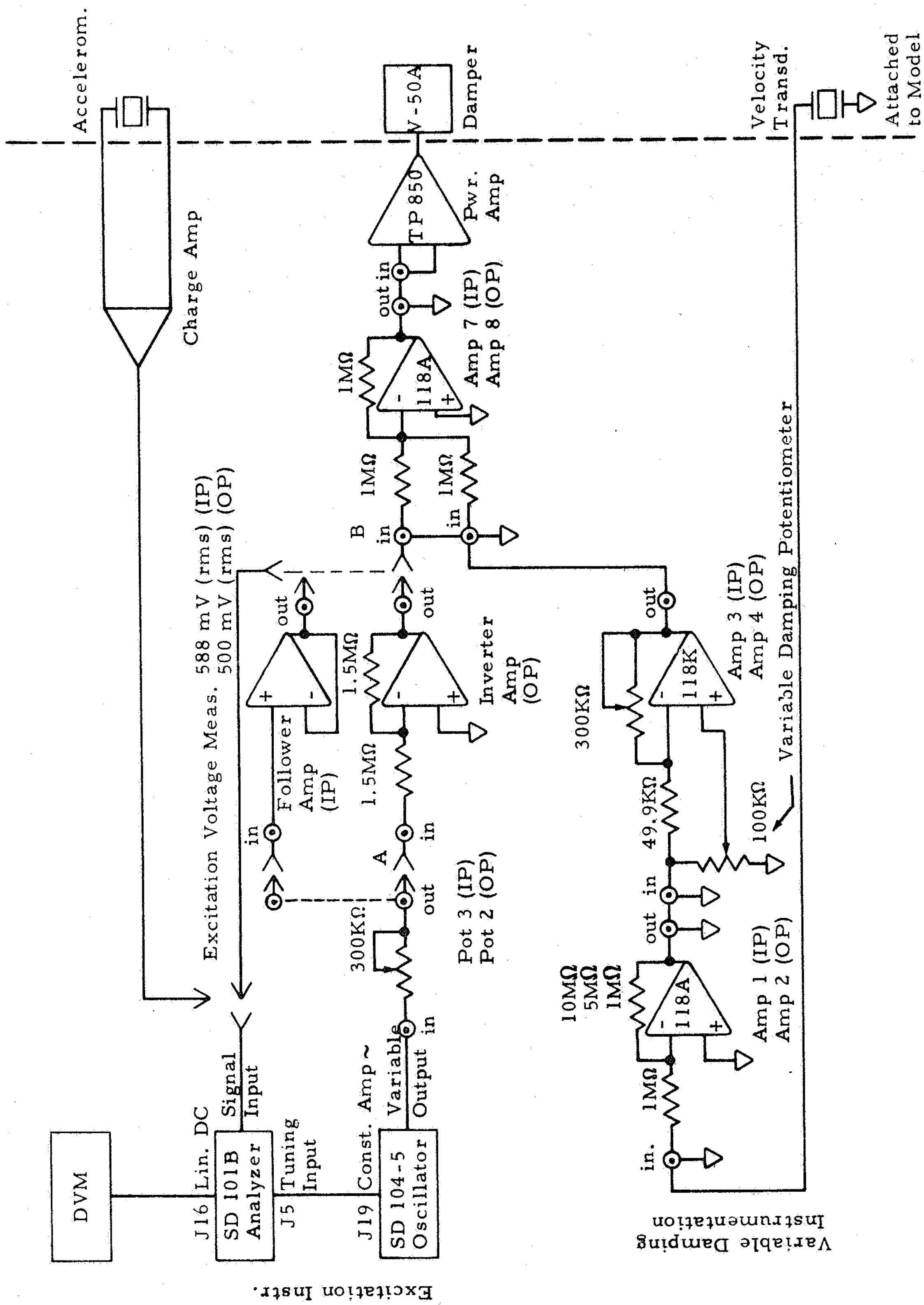

Fig. 2-2 - Damper Control and Calibration Circuit Diagram possible within the model. However, due to space limitations and, more importantly, the shaker displacement limit ($\pm$0.35 inches), the shaker package should be positioned as low as possible in the model. An obvious tradeoff decision on the shaker location was required. The final positioning is designed to guarantee a damping range $0.01 \leq \zeta \leq 0.05$ and allow unrestrained model motion over a range of response levels up to the scaled vehicle limits (see Section 3.2).

The installation of the damper in this particular position within the S-IVB stage of the model required a redesign of a set of fuel weights in order to allow clearance around the shakers. The corners of the shakers were also milled down to allow further clearance. The lead weights were molded in the shape designated in Lockheed Drawing No. R 72107, Detailed Item 41; and were installed as shown in View A of that drawing.

Section 3
DAMPER SYSTEM CALIBRATION

After the model damper mechanical components and control electronics were fabricated, assembled and checked out, the total system was transported to the Aero-Astrodynamics Laboratory at Marshall Space Flight Center to be installed and calibrated in the Saturn IB/Skylab model.

As model/damper assembly progressed, an optimum procedure was developed. The installation procedure which was used is as follows:

1. With the base pedestal secured, install the support post assembly onto the base pedestal upper flange (6, 3/8 in. -24 bolts).
2. Install first stage and align the X axis of post with X axis of model.
3. Use lifting crane to lower shaker assembly onto upper flange. Secure assembly with two bolts. Check return-to-center action of support post.
4. Lower second stage into position and thread damper instrumentation leads (two power, two load cells, and two velocity sensors) through holes in second stage lower flange.
5. Carefully lower second stage down to mate with first stage. This will require some tilting of the stage to clear shaker flexures.
6. Bolt up second stage after connecting cooling hose (see drawing) and routing leads through holes in lower flange of second stage.
7. Bolt up shaker flexures from the outside of second stage (two flat head torque-set screws for each flexure). Check alignment of shakers.

Figure 3-1 presents the radial location of the damper axes with respect to the model X and Y axes after damper installation. For additional reference the strain gage bridges axes are also indicated.

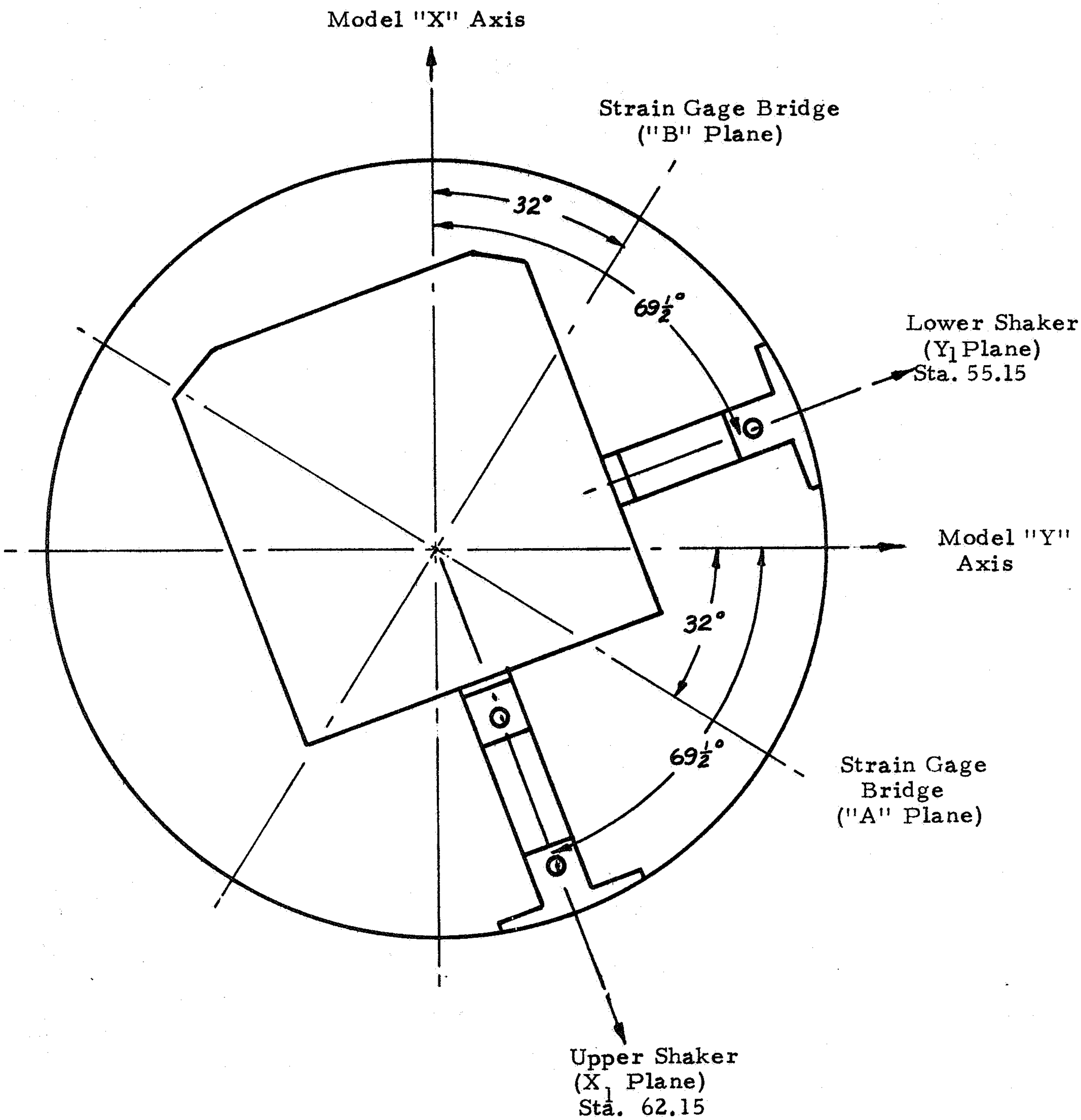

Fig. 3-1 - Saturn IB/Skylab Model - Damper Alignment

3.1 CALIBRATION OF THE DAMPER SYSTEM

Through the use of the feedback control system and a controlled oscillator input (see circuit diagram in Fig. 2-2), a range of linearly controlled viscous damping ($1.0\% \leq \zeta \leq 5.0\%$) was achieved for each of the eight model configurations. These checkout and calibration tests were performed at MSFC during June 1971. The calibration plots of Figs. 3-2 through 3-9 present the gain setting of the variable damping potentiometer (for both X1-plane and Y1-plane control circuits) as a function of the measured critical damping ratio (ζ). These measurements were made from Polaroid photographs of the free decay of the model from a reference amplitude of oscillation at first mode resonance. A summary of the conditions of each of the calibration measurements is given in Table 3-1 (page 3-12). The configuration numbers listed in Table 3-1 correspond to the following mode designations:

Configuration Number	Description
1	Empty – Primary
2	Empty – Secondary (low velocity)
3	Empty – Secondary (high velocity)
4	Intermediate – Primary
5	Intermediate – Secondary (low velocity)
6	Intermediate – Secondary (high velocity)
7	Fueled – Primary
8	Fueled – Secondary

The measured resonant frequency and the potentiometer settings for five damping levels are given in table form for each direction for each configuration on the calibration plots. Although some calibration measurements attained levels of total damping as high as 7% and even 8% for some configurations, only those settings up to 5% (the established maximum wind tunnel test level) are listed in the tables.

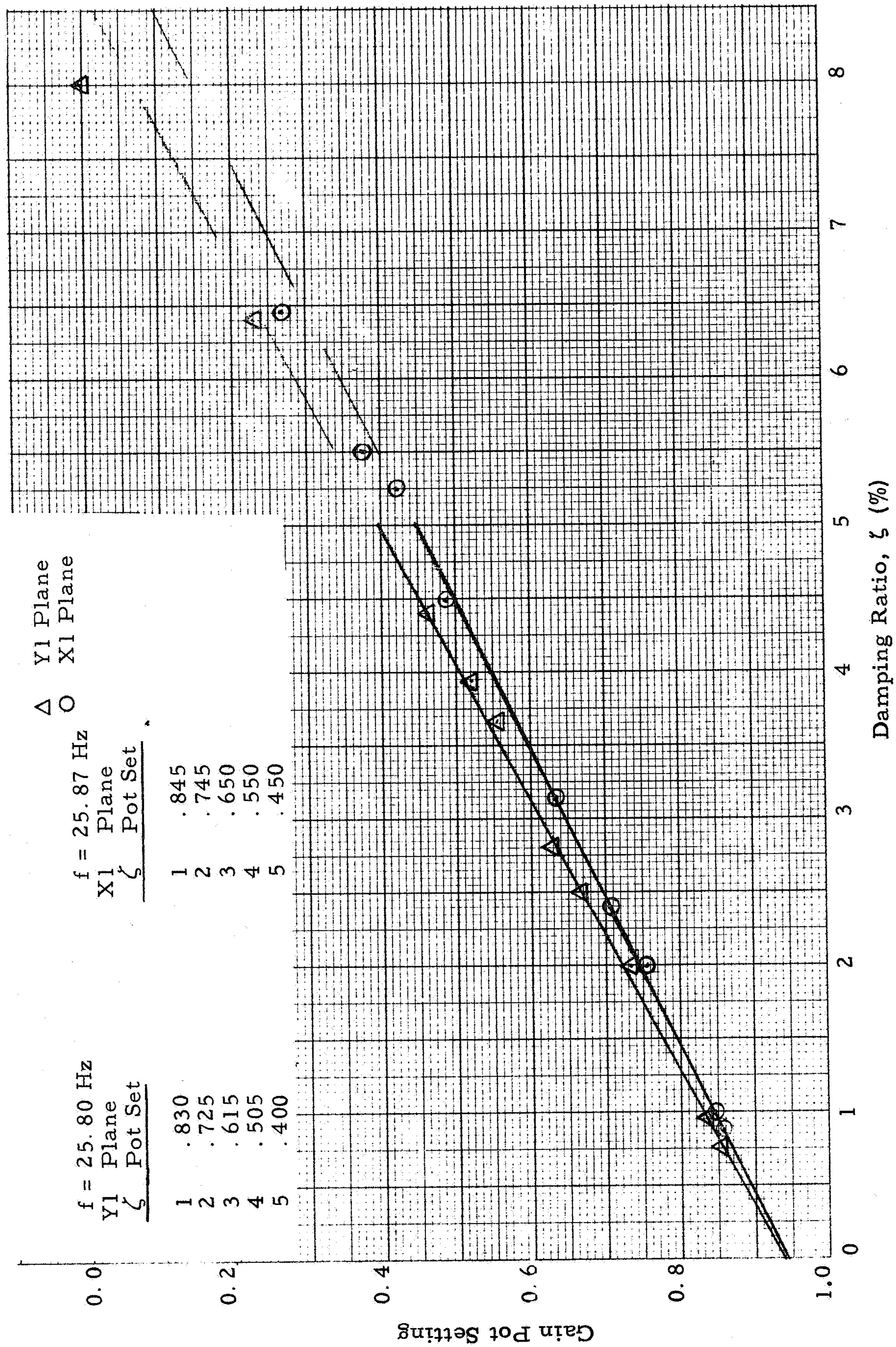

Fig. 3-2 - Damper System Calibration (Empty Primary)

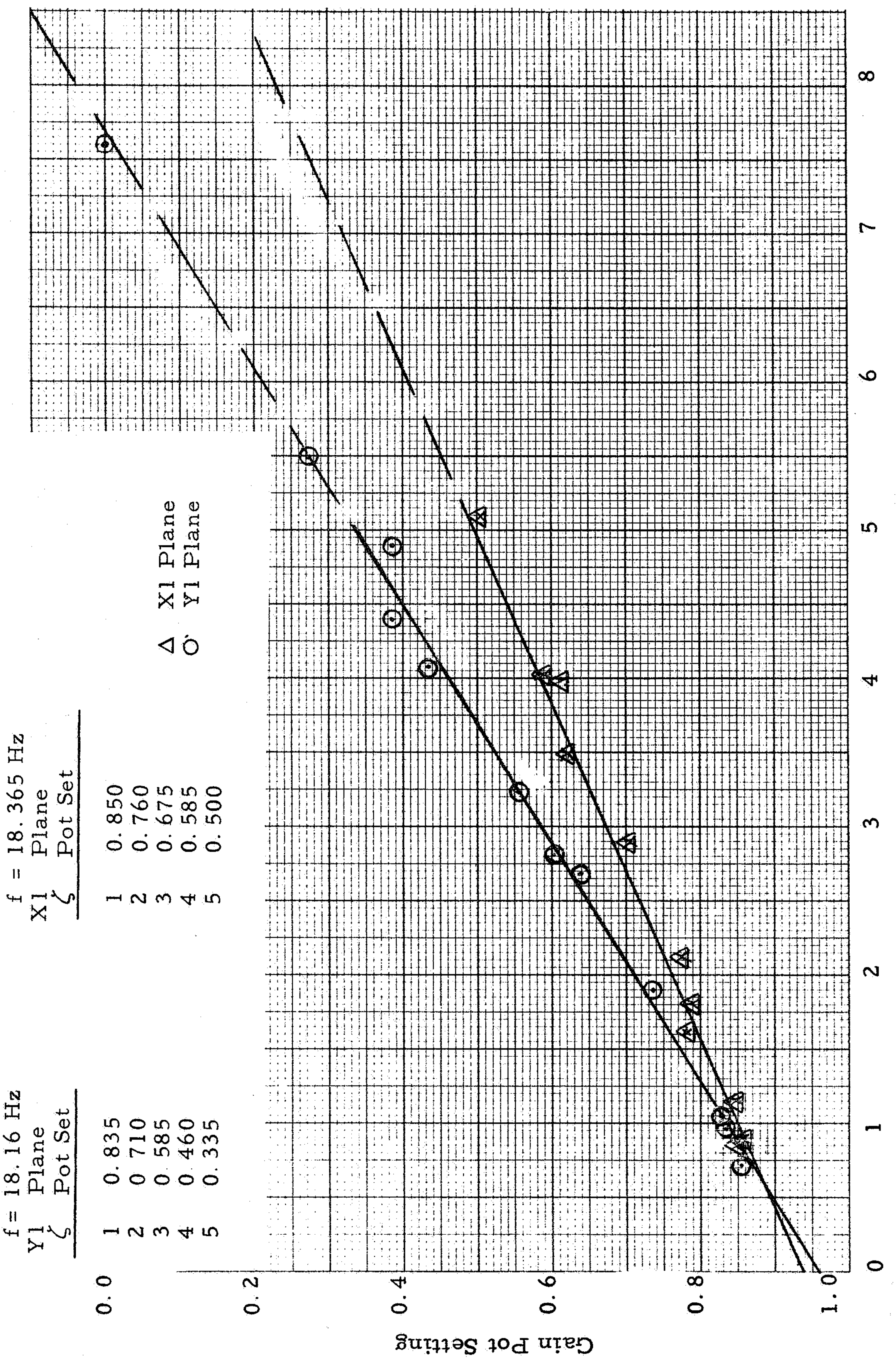

Fig. 3-3 - Damper System Calibration (Empty Secondary, Low Velocity)

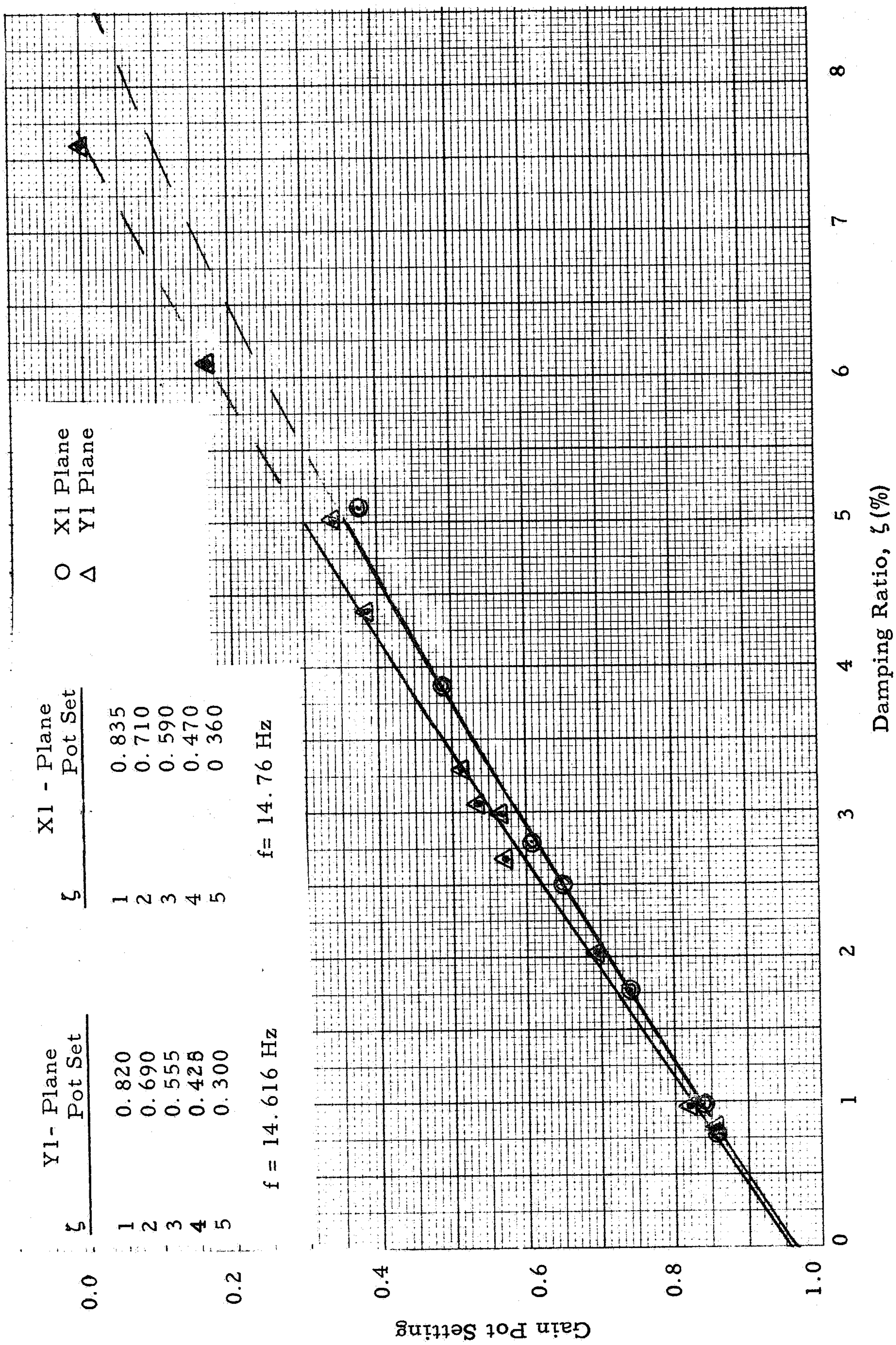

Fig. 3-4 - Damper System Calibration (Empty Secondary, High Velocity).

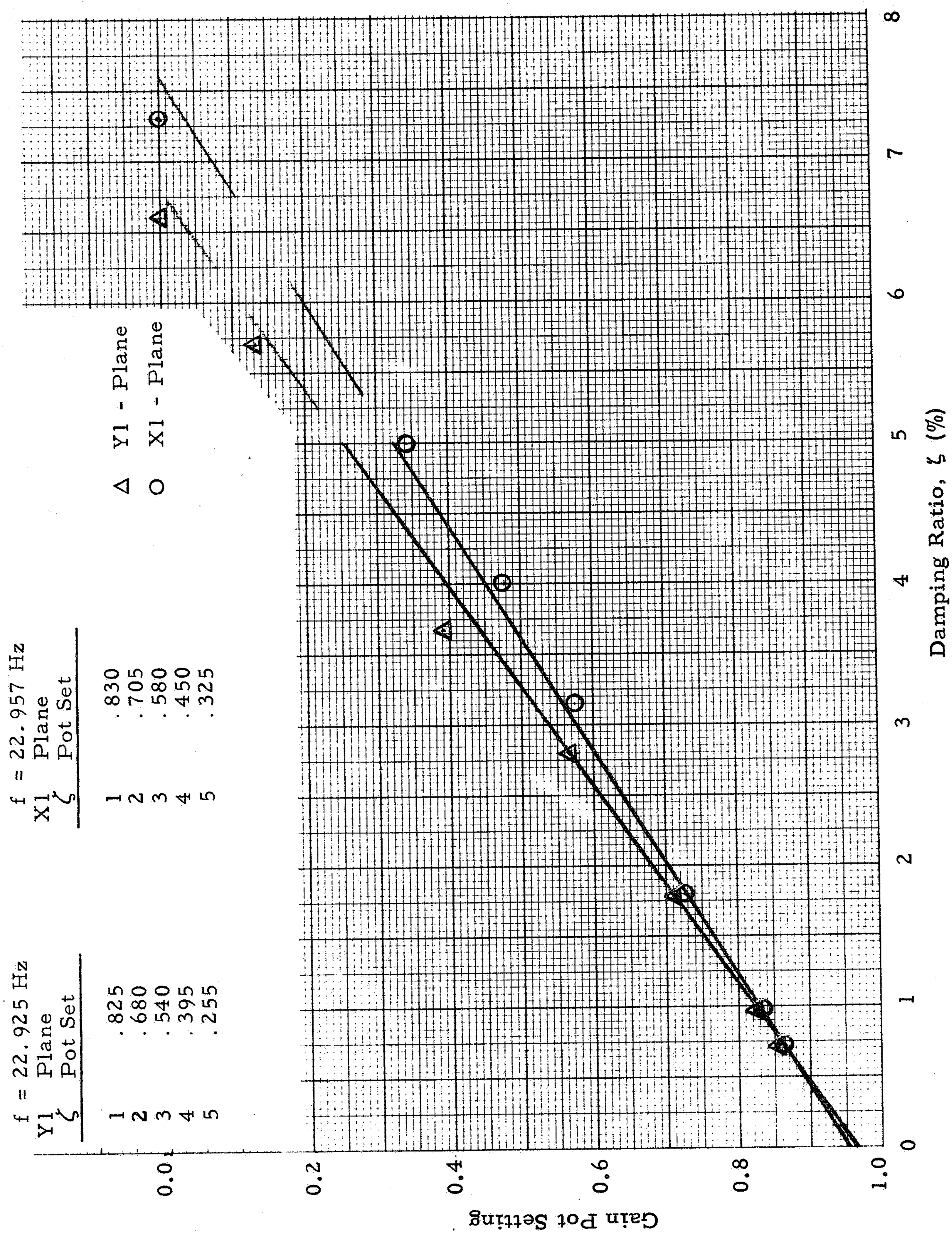

Fig. 3-5 - Damper System Calibration (Intermediate Primary)

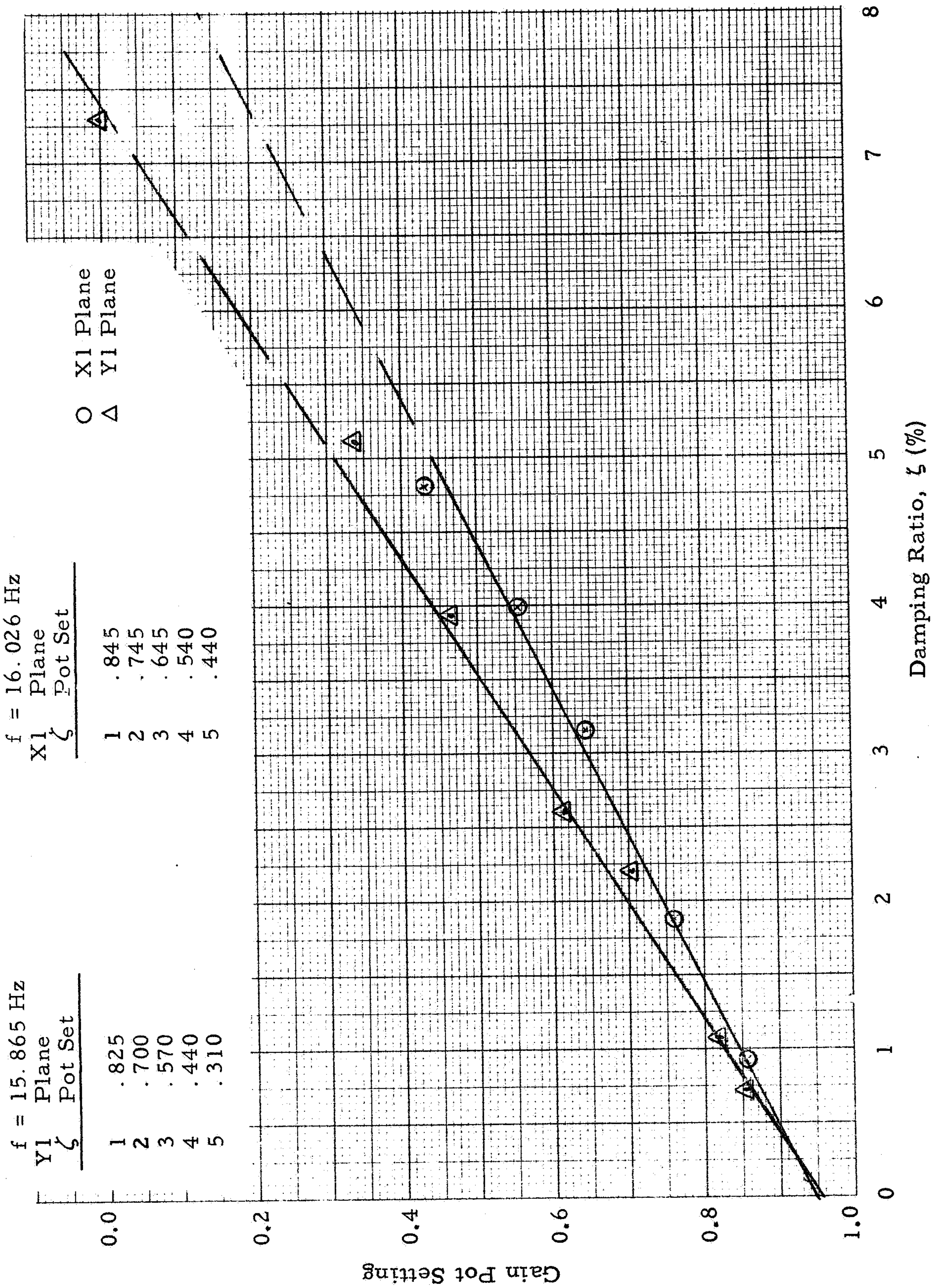

Fig. 3-6 - Damper System Calibration (Intermediate Secondary Low Velocity)

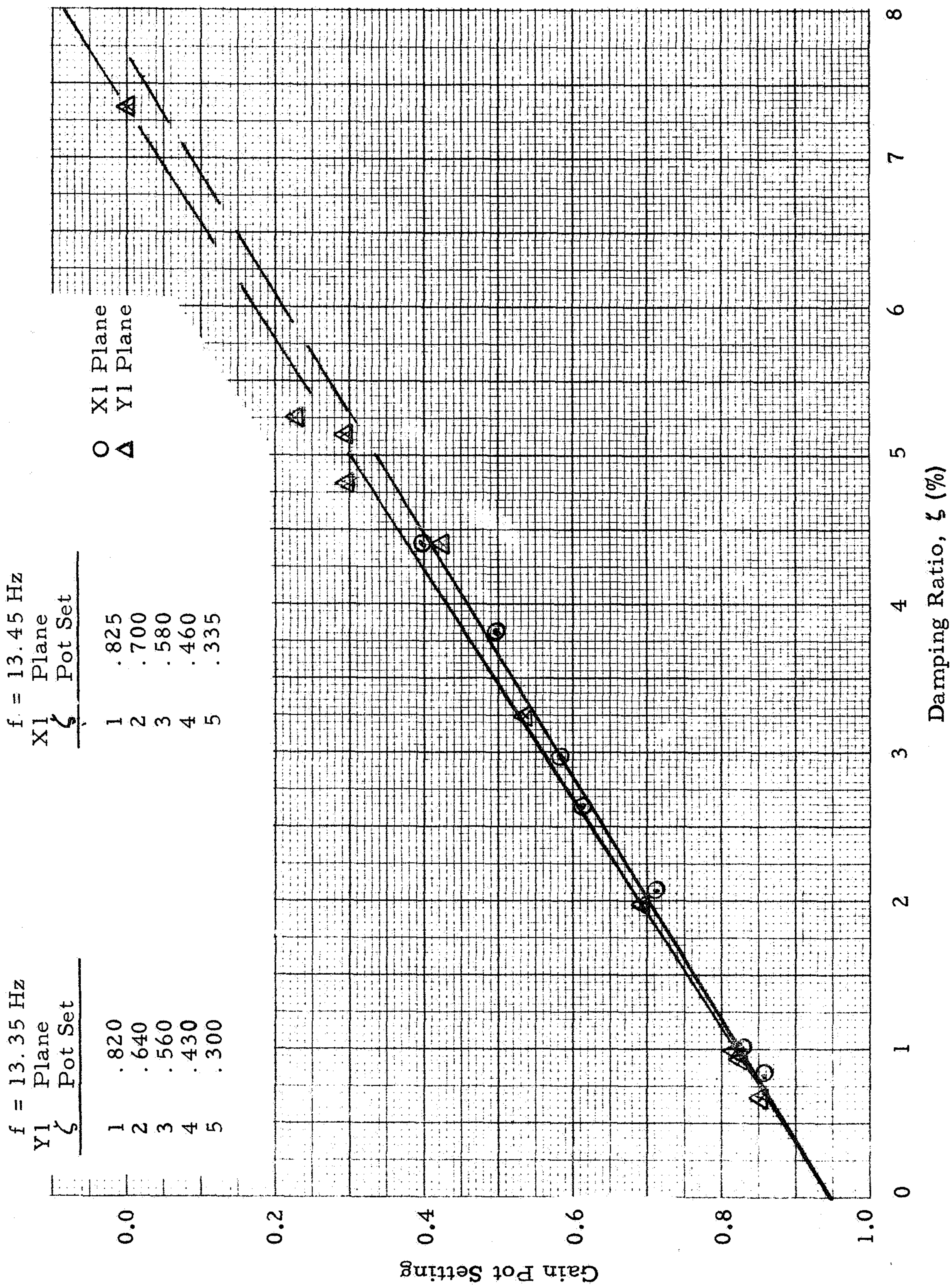

Fig. 3-7 - Damper System Calibration (Intermediate Secondary High Velocity)

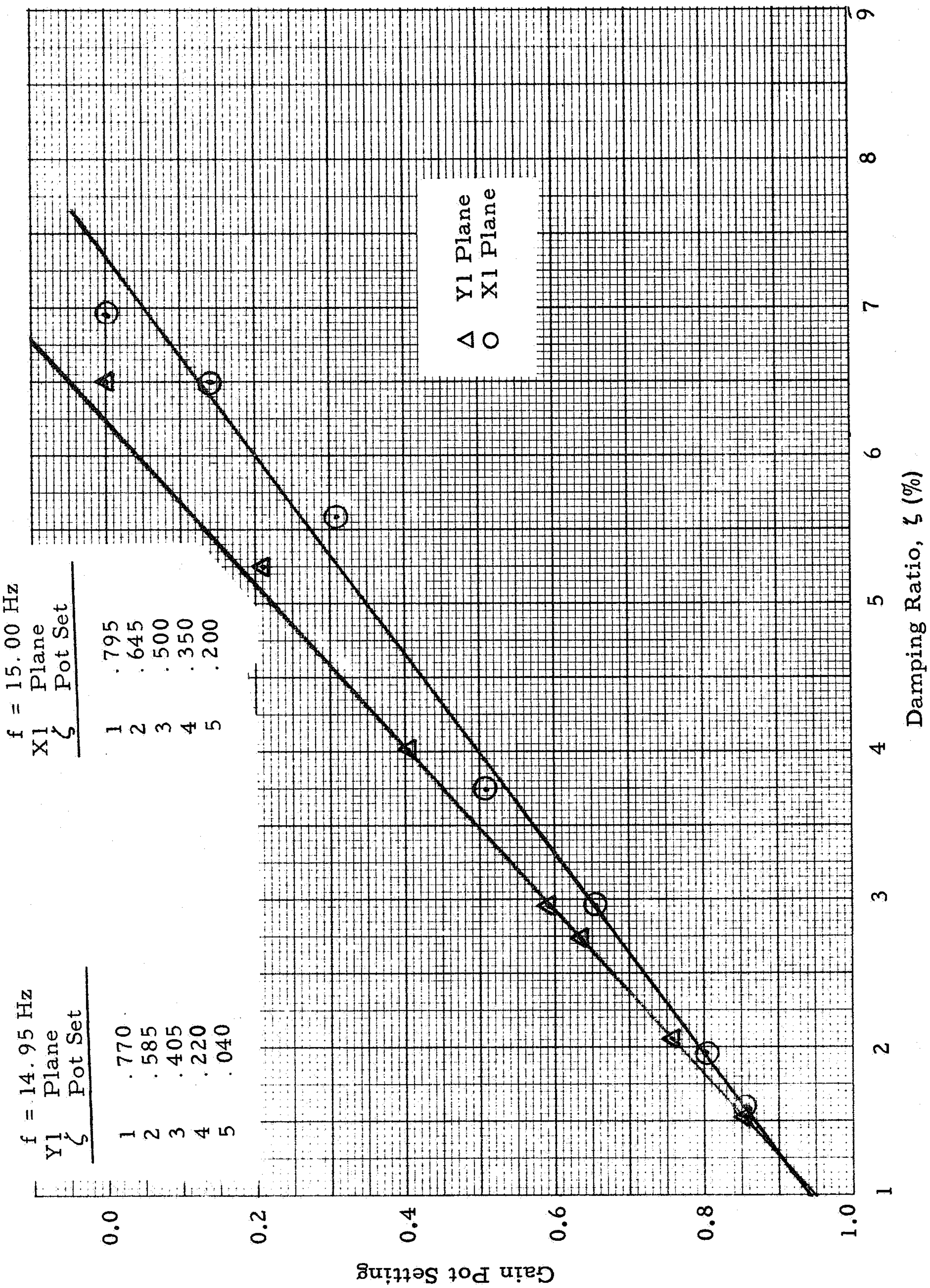

Fig. 3-8 - Damper System Calibration (Fueled, Primary)

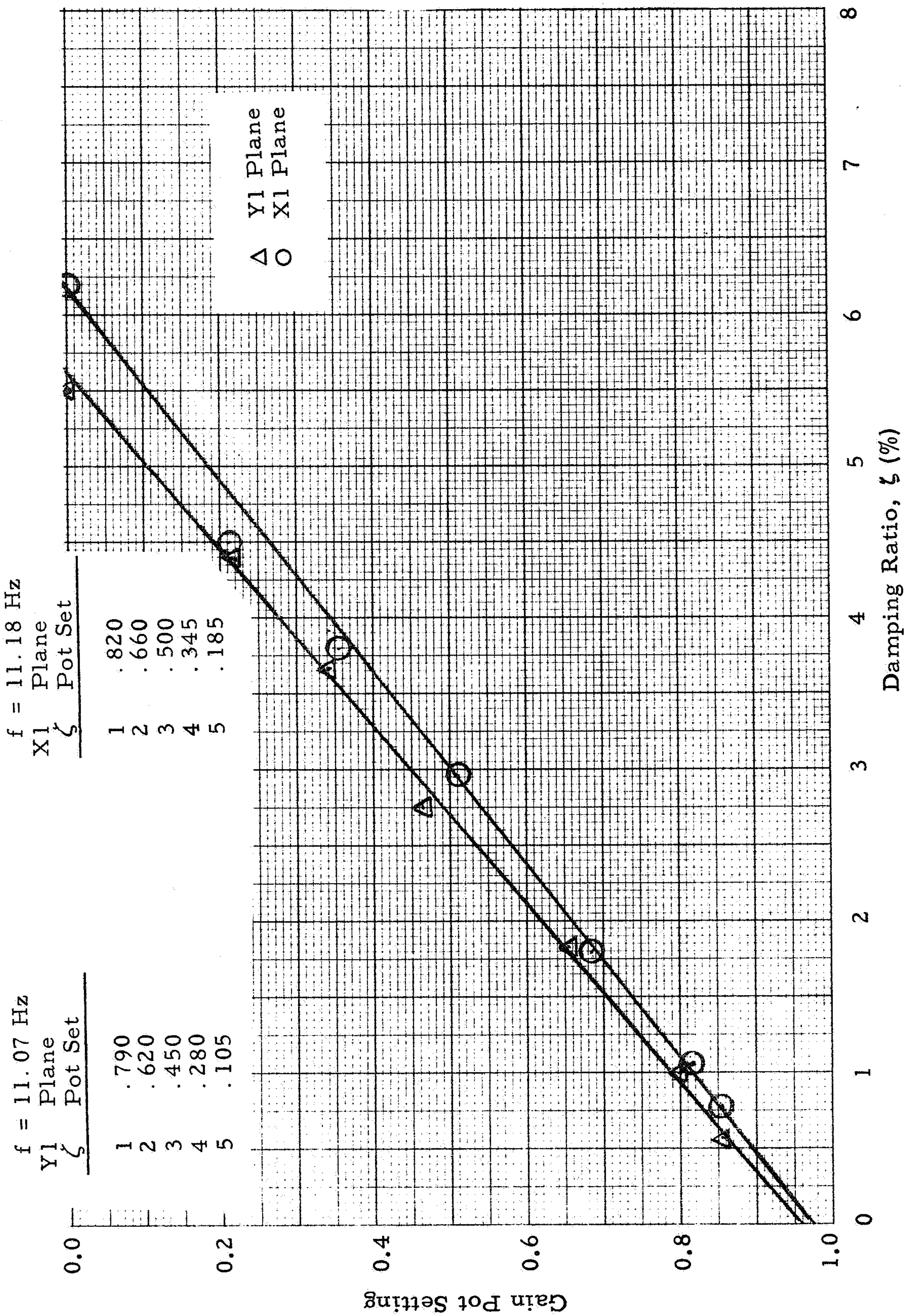

Fig. 3-9 - Damper System Calibration (Fueled, Secondary)

Table 3-1

MODEL DAMPER CALIBRATION SUMMARY

Config.	Damper Axis	Force Level (mV)	Damper Gain	Resonant Period (m sec)	Pot. Setting	Accel. Sta. 55.15 mV (rms)	Damping Factor ζ (%)
1	X1	434.0	5	38.65	.856	250	0.88
	(Upper Shaker) at 159.5° at Sta. 62.15				.845	220	1.00
					.754	110	2.00
					.705	88	2.40
					.634	68	3.14
					.525	50	4.24
					.489	46	4.50
					.426	40	5.25
					.380	36.5	5.50
					.271	31	6.45
					.000	22.2	9.15
	Y1	420.0	5	38.76	.856	250	0.76
	(Lower Shaker) at 69.5° at Sta. 55.15				.835	196	0.96
					.734	98	2.00
					.670	75	2.50
					.631	65	2.80
					.559	53	3.67
					.521	48	3.95
					.465	42	4.40
					.000	23	8.00
2	X1	467.0	5	54.50	.856	283	0.90
					.848	259	1.16
					.854	280	0.85
					.775	141	2.12
					.789	155	1.80
					.782	148	1.62
					.705	98.5	2.90
					.621	71.5	3.50
					.611	69	4.00
					.588	64	4.07
					.504	52	5.10
					.000	24	9.80

Table 3-1

Continued

Config.	Damper Axis	Force Level (mV)	Damper Gain	Resonant Period (m sec)	Pot. Setting	Accel. Sta. 55.15 mV (rms)	Damping Factor ζ(%)
2	Y1	455	5	55.10	.856	283	0.74
		455			.829	208	1.05
		455			.833	218	0.97
		478			.833	283	0.96
					.736	141.5	1.90
					.639	94.3	2.68
					.603	84.3	2.76
					.569	77.3	3.23
					.433	56.1	4.07
					.385	51.2	4.40
					.272	42	5.50
					.000	30	7.6
3	X1	465	5	67.8	.840	175	0.98
					.741	87.5	1.76
					.637	58.3	2.50
					.609	535	2.80
					.486	38.7	3.87
					.378	31.6	5.10
					.000		8.80
	Y1	441	5	68.4	.856	175	0.82
					.821	120.5	0.98
					.695	60.25	2.04
					.571	40.1	3.00
					.516	34.7	3.29
					.388	27.2	4.40
					.343	25	5.00
					.172	19.6	6.30
					.000	16	7.60

Table 3-1
Continued

Config.	Damper Axis	Force Level (mV)	Damper Gain	Resonant Period (m sec)	Pot. Setting	Accel. Sta. 55.15 mV (rms)	Damping Factor ζ (%)
4	X1	434.4	5	43.56	.856	220	0.76
					.832	170	0.96
					.726	85	1.80
					.575	50	3.15
					.472	39	4.00
					.342	31	5.00
					.000	19.6	7.30
	Y1	419.5	5	43.62	.856	220	0.71
					.827	161	0.98
					.716	80	1.80
					.569	48	2.81
					.389	32	3.67
					.131	22	6.10
					.000	19	6.60
5	X1	440	5	62.4	.856	175	0.92
					.762	80	1.86
					.646	48	3.15
					.554	36	4.00
					.432	28	4.80
					.000	15.3	8.80
	Y1	432	5	63.03	.856	175	0.73
					.821	120.3	1.07
					.705	60.1	2.20
					.616	44	2.60
					.466	30	3.94
					.342	24	5.12
					.000		7.30

Table 3-1

Continued

Config.	Damper Axis	Force Level (mV)	Damper Gain	Resonant Period (m sec)	Pot. Setting	Accel. Sta. 55.15 mV (rms)	Damping Factor ζ (%)
6	X1	460.7	5	74.33	.856	175	0.82
					.828	133	1.02
					.712	66.5	2.06
					.614	47	2.63
					.585	43	2.98
					.496	34	3.80
					.396	28.3	4.40
					.000		6.87
	Y1	435.2	5	74.90	.856	150	0.69
					.829	110	0.92
					.820	101	1.00
					.696	50.5	2.00
					.537	30.9	3.25
					.423	24.3	4.40
					.296	19.4	5.14
		480			.296	33	4.80
					.220	29.0	5.25
					.000	22	7.35
7	X1	461.4	5	66.65	.856	200	0.61
					.802	122	0.97
					.658	61	1.96
					.509	40	2.75
					.311	27.5	4.60
					.147	22	5.50
					.000		5.95

Table 3-1

Continued

Config.	Damper Axis	Force Level (mV)	Damper Gain	Resonant Period (m sec)	Pot. Setting	Accel. Sta. 55.15 mV (rms)	Damping Factor ζ(%)
7	Y1	448.2	5	66.90	.856	200	0.54
					.643	55	1.75
					.760	93	1.05
		463	5		.760	110	0.95
					.595	57.5	1.96
					.406	37	3.01
					.210	27	4 25
					.000	21	5.50
8	X1	459	5	89.40	.856	125	0.74
					.816	98.5	1.05
					.685	49.3	1.80
					.510	29.5	2.96
					.357	22.2	3.80
					.211	17.5	4.50
					.000		6.20
	Y1	442.5	5	90.30	.856	143	0.56
					.797	82.8	1.00
					.653	41.4	1.83
					.465	25.3	2.75
					.345	19.9	3.66
					.214	16.5	4.40
					.000	12.7	5.50
		501.5			.000	25	5.50

3.2 PREDICTED MODEL DAMPER CAPABILITIES

The operational limits of the model damper system as installed in the 5.5% Saturn IB/Skylab model can be computed from model dynamic characteristics and approximations of the expected aerodynamic loading. The following computations are based on model ideal characteristics as supplied on 26 January 1971 by S&E-AERO-AU; thus, these data do not necessarily represent the final (as constructed) test model characteristics. Only two model configurations will be considered here since damper performance characteristics for these two extreme cases will bracket the values for the other model configurations.

Model Dimensions and Limit Moment

Base strain gage bridge level = Sta. 11.18
Model tip station level = Sta. 147.40
Original model design maximum moment (red-line) = 2.0×10^5 in. -lb at Sta. 11.18

Empty Model Characteristics

First mode frequency (f_1) = 24.6 Hz
First mode generalized mass (GM_1) = 0.0391 lb-sec^2/in.
Base (Sta. 11.18) modal moment (BM_1) = 170,605 in. -lb/in. (tip)
Mode shape (ϕ_1) at Sta. 55.15 = 0.253
Mode shape (ϕ_1) at Sta. 62.15 = 0.293

Fully Fueled Model Characteristics

First mode frequency (f_1) = 15.106 Hz
First mode generalized mass (GM_1) = 0.1599 lb-sec^2/in.
Base (Sta. 11.18) model moment (BM_1) = 220,409 in. -lb/in. (tip)
Mode shape (ϕ_1) at Sta. 55.15 = 0.340
Mode shape (ϕ_1) at Sta. 62.15 = 0.382

The peak response amplitude at the upper shaker flexure (Sta. 62.15) with the model oscillating at the expected maximum base moment of 2.0×10^5 in. -lb at Sta. 11.18 is

$$X_{62.15} = \frac{200,000}{BM_1} \phi_{62.15}$$

which for the empty case is 0.3435 inches and for the fueled case is 0.3466 inches. Thus, the peak expected shaker coil displacements are within the maximum stroke capability ($\pm$0.35 inches) of the Ling (Goodmans) V-50A shakers.

In order to determine the maximum allowable aerodynamic load which the model/damper system can sustain at peak shaker loads, we consider the following: Under a steady state oscillation condition

$$\text{Total Damping Force} = \text{Excitation Force} = F_a + F_i$$

where

F_a = the additive damping force imparted by the shaker

F_i = the inherent equivalent damping force of the model (parasitic structural damping)

then, since

$$\frac{\zeta_i}{\zeta_a} = \frac{F_i}{F_a}$$

where ζ_i is assumed to be 0.01 and ζ_a must then be 0.04 (in order to achieve a total damping level of ζ_T = 0.05), then we have

$$F_a \left(1 + \frac{F_i}{F_a}\right) = F_a \left(1 + \frac{\zeta_i}{\zeta_a}\right)$$

or

$$\text{Maximum Excitation Force} = 1.25\ F_a$$

And, thus, with the 50-pound capability of the Ling V-50A shaker, the system can produce a total damping coefficient of 5% for all aerodynamic excitation force levels up to 62.50 pounds. This aerodynamic force is equivalent to an allowable maximum generalized force at the tip of the model (Sta. 147.4) of

$$GF\ (\text{tip}) = \phi_1\ (\text{Sta. } 55.15) \times 62.5$$

where the lower shaker station is considered since it yields a lower maximum level. This maximum is 15.81 lb for the empty case and 21.25 lb for the fueled case.

Assuming a steady state sinusoidal excitation of the above amplitudes at model first mode resonance, the dynamic bending moment amplitude can be expressed as follows.

$$DBM_{11.18} = BM_1 \left\{ F_o / 2\zeta\ (GM_1)\, \omega_1^2 \right\}$$

which yields the expected model base bending moment for $\zeta_T = 0.05$ under the influence of the above dynamic loads. These resultant moments are 28,905 in.-lb for the empty case and 32,574 in.-lb for the fueled case.

The same forcing function will drive the model to the design (red-line) limit of 2.0×10^5 in.-lb at Sta. 11.18 if the total damping ratio (ζ_T) is

$$\zeta_T = \frac{BM_1 \times GF\ (\text{tip})}{(2.0 \times 10^5)\ 2(GM_1)\,\omega_1^2}$$

which for the empty model is 0.007 and for the fueled model is 0.008. These damping ratios are lower than those planned for the testing conditions; therefore, the damper system is capable of supplying a range of total damping of

$$0.007 \leq \zeta_T \leq 0.05$$

for the aerodynamic loads considered above.

Approaching the operational limits in a somewhat different way we may ask: "With the shakers operating at peak stroke (± 0.35 inches) what is the allowable base bending moment response and what is the corresponding maximum tip displacement of the model?" The dynamic base bending moment under such conditions would be

$$DBM_{11.18} = BM_1 \left(\frac{0.35}{\phi_1 \text{ (Sta. 62.15)}} \right)$$

which becomes 203,793 in.-lb for the empty case and 201,945 in.-lb for the fueled case. The corresponding tip displacements can be expressed as

$$X_{147.3} = \frac{0.35}{\phi_1 \text{ (Sta. 62.15}}$$

which for the empty case is ± 1.193 inches and for the fueled case is ± 0.916 inches.

This completes the determination of predicted model damper operational capabilities.

Section 4
WIND TUNNEL TEST SETUP AND INSTRUMENTATION

The entire model damper system, including all mechanical components, control console, wiring, and tools, was transported to Langley Field, Virginia, for the ground winds test of the Saturn IB/Skylab 5.5% model. The Transonic Dynamics Tunnel (TDT) was used for the tests. Langley project leaders were Tom Foughner and Bob Hess. MSFC project leaders were Richard Beranek and Jim Poe. TDT Test No. 200 was assigned to the program; and, after a short delay for tunnel maintenance work, instrumentation planning and model installation and checkout were performed.

The model damper installation in the Saturn IB/Skylab model at the wind tunnel was to be identical with the procedure outlined previously with the additional requirement that the shaker power leads and the damper instrumentation leads were to be routed through the model turntable and back to the instrumentation room (a distance of approximately 40 feet). Cables were provided for all six leads plus two more for the tip accelerometers. In addition, a full set of strain gage cables was provided for the model-associated strain instrumentation.

The operational procedure after the installation and connection of the model damper and its control system is the following:

1. Ensure proper polarity of damper control/velocity sensor/ shaker in the closed loop.
2. Ensure that circuit is closed to the input of each power amplifier and that input level is zero before turn-on procedure is attempted.
3. Power amplifier turn-on procedure: Make sure that gain control is fully CCW, then throw toggle switch to STANDBY. Then, immediately throw circuit breaker (amplifier) switch to ON.

4. Amplifier is now ready for gain control to be brought up to maximum level (full CW). Note: All damper calibrate levels have been measured with gain controls (both amplifiers) at full CW.

5. Select the proper gain setting for each of the variable damping potentiometers from the calibration chart and set the level into each pot. Check damping in both in-plane and out-of-plane directions and at least one off-angle direction. The system is then ready for testing.

Since the model damper system was scheduled to provide a totally operational and calibrated backup for the primary damper system, our efforts were directed toward support of the total model system and its preparation for testing. Tip accelerometer instrumentation cables were installed with each stage of the model. Routing of the long (about 40 feet) test station-to-model lead wires was then begun. The model instrumentation was integrated into the Langley data acquisition system and a preliminary calibration of the model strain gages was performed.

Initial problems developed with the primary damper system; and, after the loss of use of one of the power amplifiers of that system, the TP-850 Ling power amplifiers were substituted in the excitation circuit and used for the initial model dynamic calibration.

Early wind-on testing resulted in some structural failures in the joints on the model Launch Umbilical Tower. Assistance was given in the design and preparation of bolt-on reinforcements. During all stages of model testing (which included dual-shift operations) Lockheed personnel assisted in data acquisition, model configuration changes, and test monitoring. Figure 4-1 is a diagram of the model and wind tunnel instrumentation, signal conditioning and recording equipment used during the model testing. Time-lapse photographs of the base strain gage bridge outputs were taken at the "Scope-Camera" station within the instrumentation room. These photos were retained by Langley Research Center. Data tape recordings were made of model response signals in the format given in Table 4-1. The channel identification shown was retained for all test cases. Both ac and dc calibration signals were recorded on all sensor channels on each reel of tape.

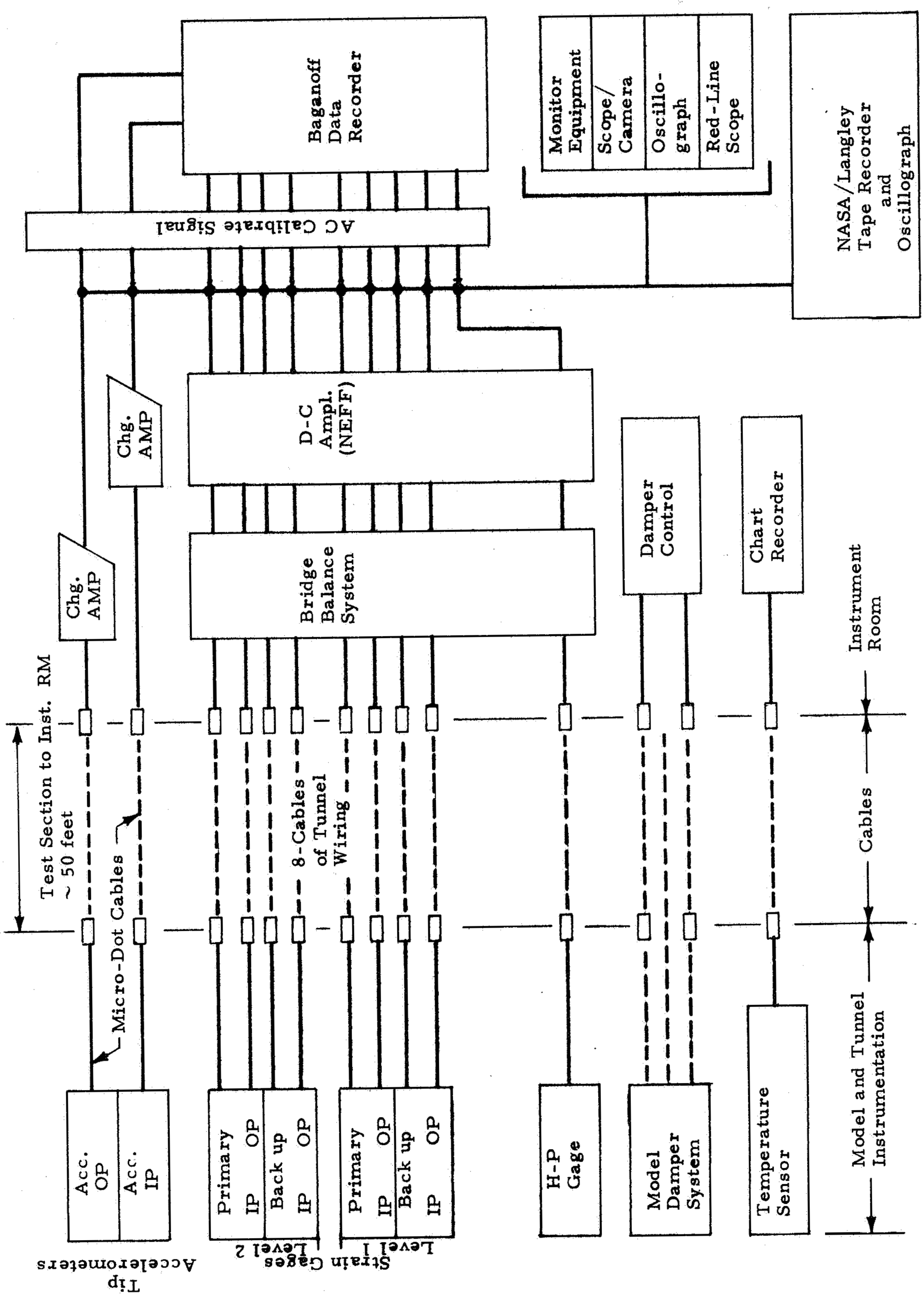

Fig. 4-1 - Instrumentation Diagram Saturn IB/Skylab Test

Table 4-1

TAPE RECORDER CHANNEL IDENTIFICATION

Channel Number	Signal
1	Strain Gage Bridge 1A (Sta. 11.18)
2	X-Axis Acceleration (Sta. 90)
3	Strain Gage Bridge 1B (Sta. 11.18)
4	Y-Axis Acceleration (Sta. 90)
5	Strain Gage Bridge 2A (Sta. 59.25)
6	Blank
7	Strain Gage Bridge 2B (Sta. 59.25)
8	Blank
9	X-Axis Acceleration (Model tip)
10	Blank
11	Y-Axis Acceleration (Model tip)
12	Blank
13	Wind Tunnel Dynamic Pressure (H-P)
14	Voice Identification (Direct Record)

Section 5
WIND TUNNEL DATA REDUCTION

Tape recordings of selected test data points were provided to Lockheed by S&E-AERO-AU for developing power spectral analyses of certain of the model response signals. These tape reels were duplicates of the wind tunnel recordings and were recorded in the format listed in Table 4-1.

An analog signal analysis system was set up in the instrumentation room at the Structures Laboratory at Lockheed-Huntsville. Figure 5-1 is a block diagram of that system. The components used are as follows:

Sweep Oscillator	Spectral Dynamics Model SD-104A-5
Dynamic Analyzer	Spectral Dynamics Model SD-101A With Carrier Amplifier Model SD-34
Tracking Filter	Spectral Dynamics Model SD-1012B
X-Y Recorder	Hewlett-Packard Model 7000A

The Dynamic Analyzer in conjunction with the Carrier Amplifier provides a 2.4-volt peak-to-peak 100 kHz carrier signal to the Tracking Filter. This carrier signal carries the sinusoidal tuned output of the sweep oscillator. The tracking filter acts as a dual-channel bandpass filter in which the center frequency of the selected passband is continuously tuned to track the frequency of the sweep oscillator. By this method the average power within the passband can be continuously generated within the tracking filter as it is swept over the

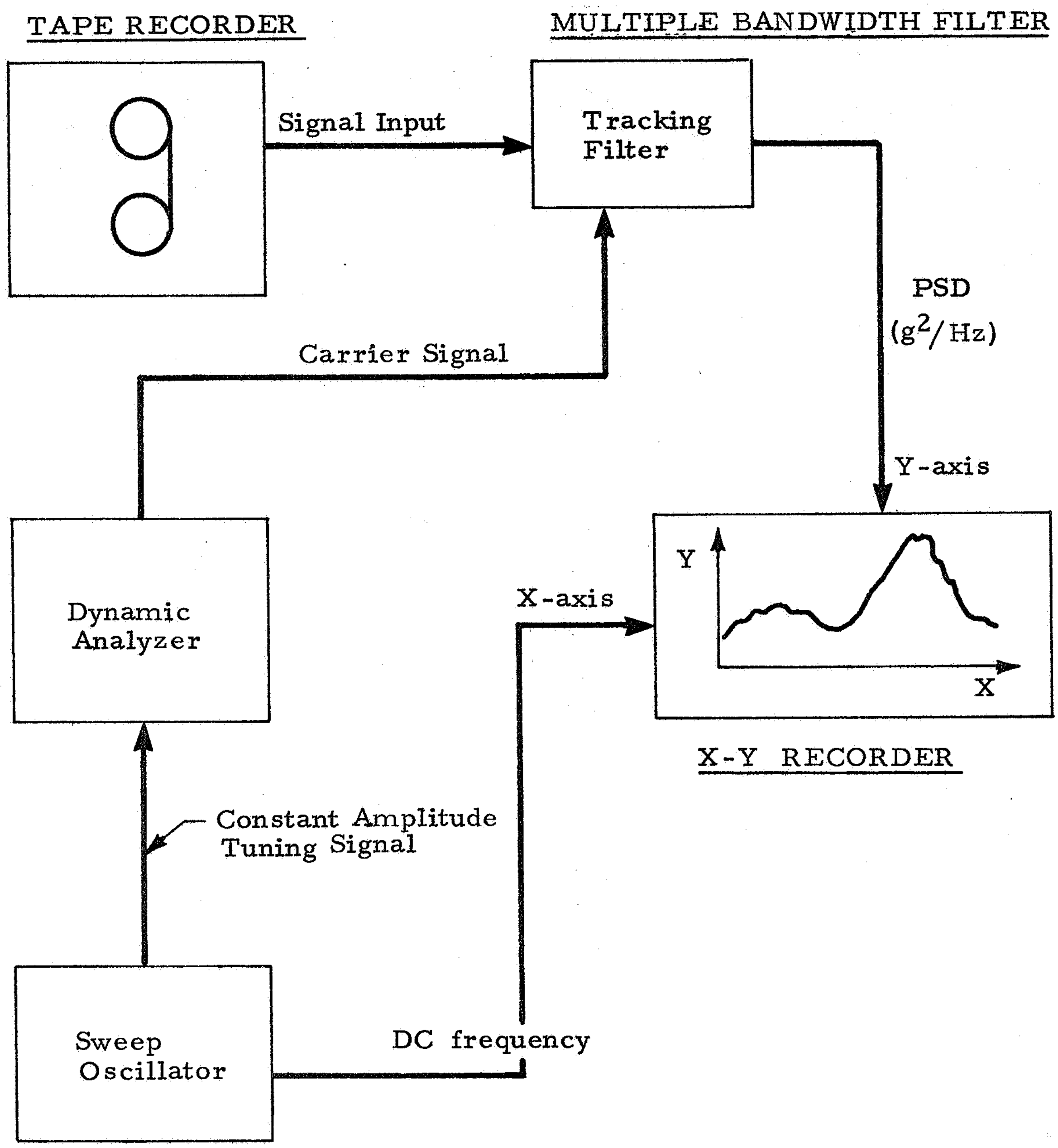

Fig. 5-1 - Diagram of PSD Analysis System frequency range of interest. The tracking filter is fitted with two constant-bandwidth filters with an automatic frequency crossover at 100 cps. Filter 1 (with a bandwidth of 2 Hz) is operative from 10 Hz up to 100 Hz where the the crossover switches to Filter 2 (with a bandwidth of 20 Hz). Thus, the spectral analysis system furnishes a complete spectrum analysis from 10 Hz to 400 Hz with automatic switching of filter bandwidths, averaging time constant and sweep rate (controlled by the oscillator). This frequency range includes both first- and second-beam modes of the model in each of its configurations. The data tapes used include the following test data points:

Data Point	Description
92	Empty-Secondary Configuration Sweep data from q = 20 psf to q = 180 psf Damping = 1.0% Wind azimuth = 105° Duration = 5 minutes
95	Empty-Secondary Configuration Sweep data from q = 20 psf to q = 180 psf Damping = 1.0% Wind azimuth = 120° Duration = 5 minutes
210 through 219	Intermediate-Secondary Configuration Dwell data at dynamic pressures varying from 50 psf to 120 psf Damping = 1.0% Wind azimuth = 105° and 120° Duration = about 1 minute for each dwell

Figures 5-2 through 5-6 present the logarithmic output of the tracking filter (the power spectral density) for the analysis of the 1A (Sta. 11.18) Strain Gage Bridge signal for the data points indicated. Because of the short running time of the dwell data points, some switching transients appear in the output.

These "spikes" were caused by tape recorder shutoff and rewind and should thus be disregarded for data interpretation purposes. Required filter (oscillator) sweep rates dictated this stop-rewind-replay procedure in order to complete the investigation over the frequency range of interest. It should be noted that, for each of the sweep data points (92 and 95), another PSD is presented (92-down and 95-down). This PSD is for the identified response signal recorded as the wind tunnel dynamic pressure was reduced from the maximum (180 psf) level. Unless otherwise indicated, all other sweep data PSD plots are an analysis of the response signal during the controlled q-ascent portion of the test. Also two plots are shown on the sweep data analysis. Plot 1 presents the PSD response for which the frequency sweep began at 20 psf and Plot 2 is the PSD of response corresponding to a passage of the sweep frequency through model resonance near the same instant the model response reached a maximum. Small tick marks in the left margin of the plots indicate the relative PSD of the tape head noise (no signal) prior to the start-up of the PSD analysis.

Figures 5-7 through 5-11 are the PSD of the 2A (Sta. 59.25) Strain Gage Bridge signal output. Only data points 215 and 216 are presented from the dwell data. These plots indicate the presence of second mode response (although approximately 60-80 dB down) in the vicinity of 100 Hz.

Figures 5-12 through 5-15 present the results of analysis of the Sta. 90 acceleration signal (in the X-axis direction). Since Sta. 90 is very near the second mode nodal point no significant energy level is noted at 100 Hz.

Figures 5-16 through 5-20 are the PSD analyses of the model tip (Sta. 121) acceleration signals (X-axis direction) for each of the data points. These PSD plots show a more active participation of the second and third modes in the model response.

Figure 5-21 is a plot of the PSD of the constant amplitude ac -calibration signal on the tape. It is presented for comparison purposes; and, as can be seen from the peak curve shape, accurately presents the PSD of the sine wave by revealing the 2 Hz bandwidth filter characteristic at 3 dB down from the peak.

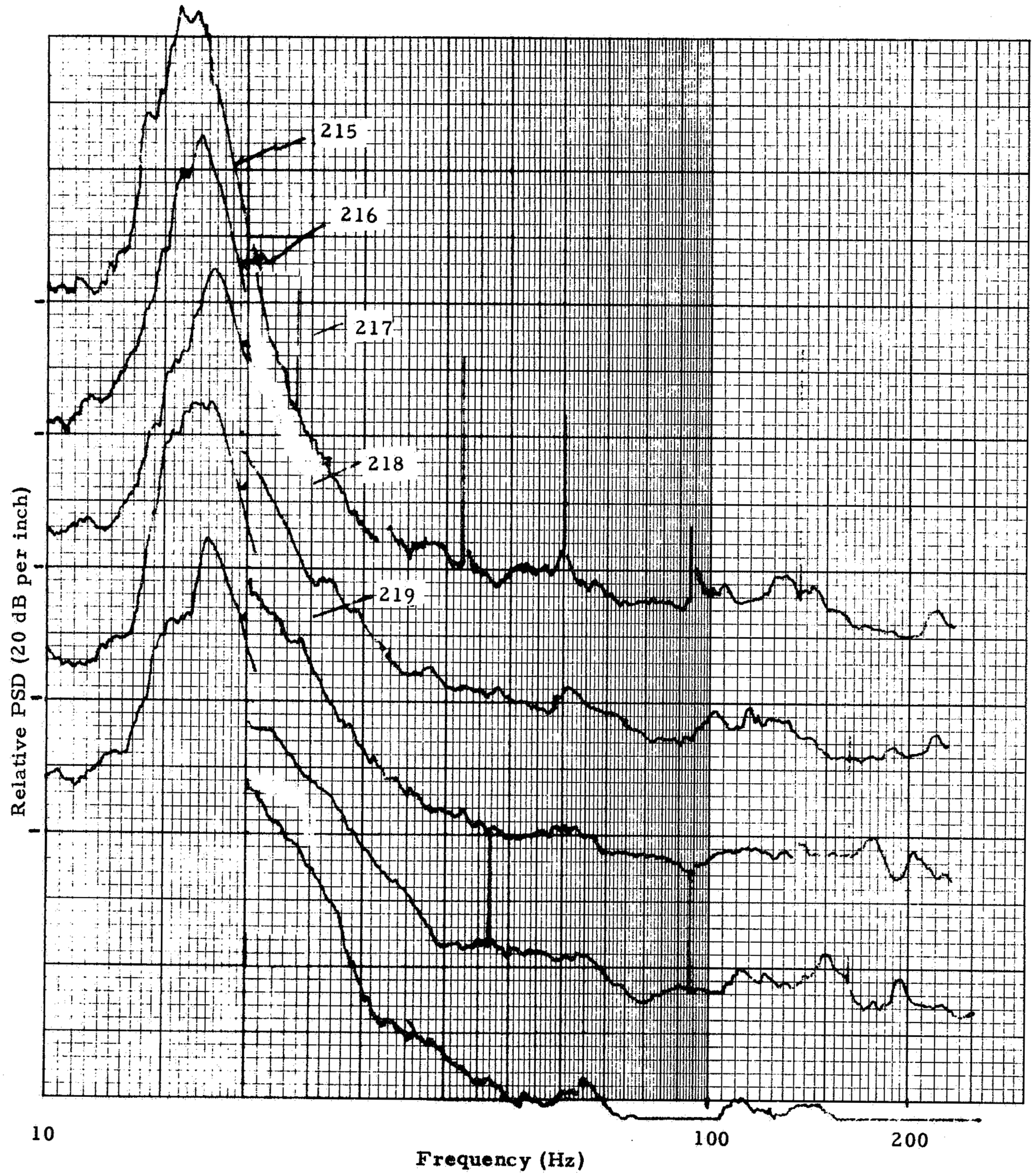

Fig. 5-2 - Dwell Data Points 215 Through 219 — Base Bending Moment (1A)

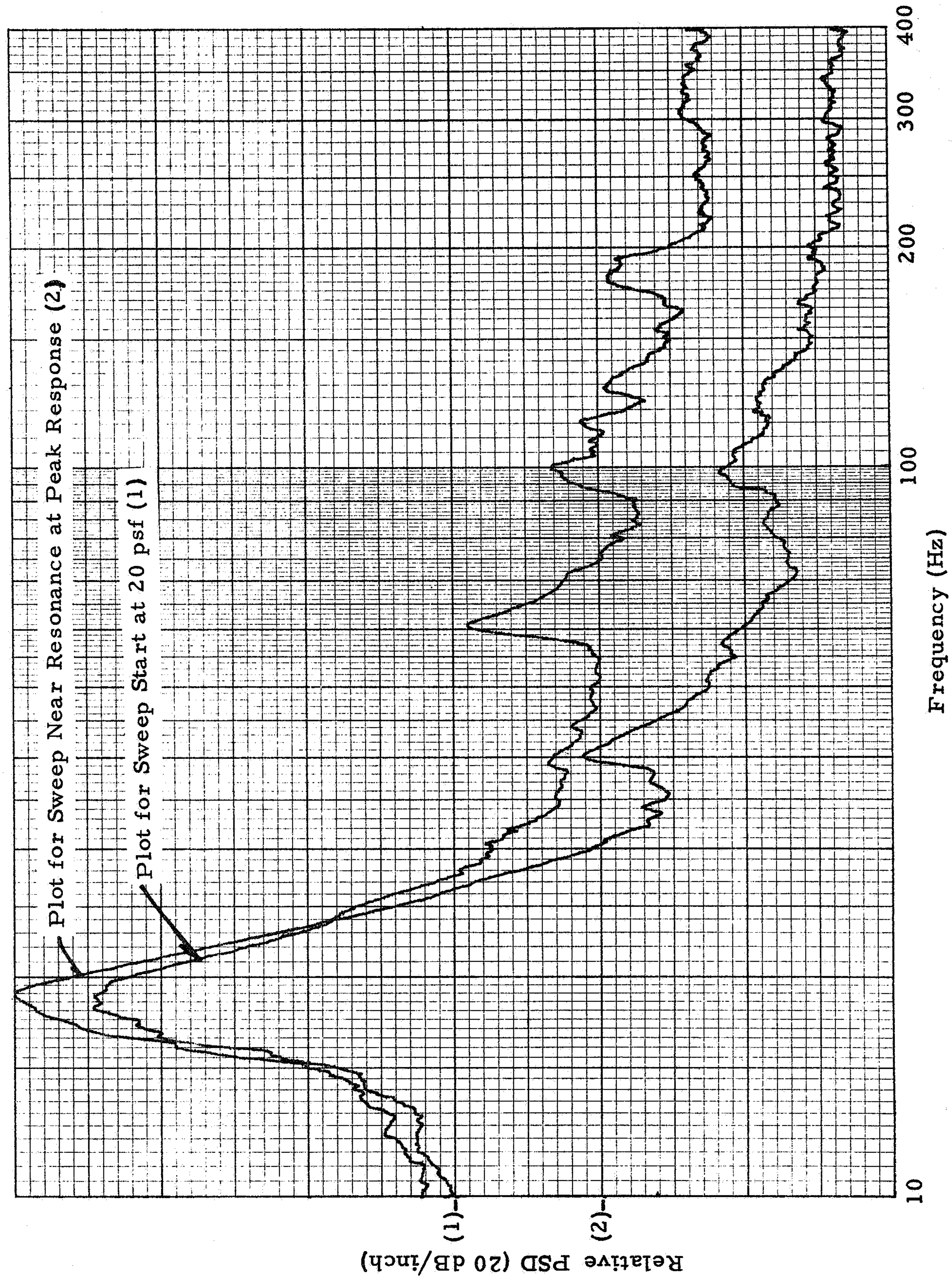

Fig. 5-3 - Sweep Data Point 92 — Base Bending Moment (1A)

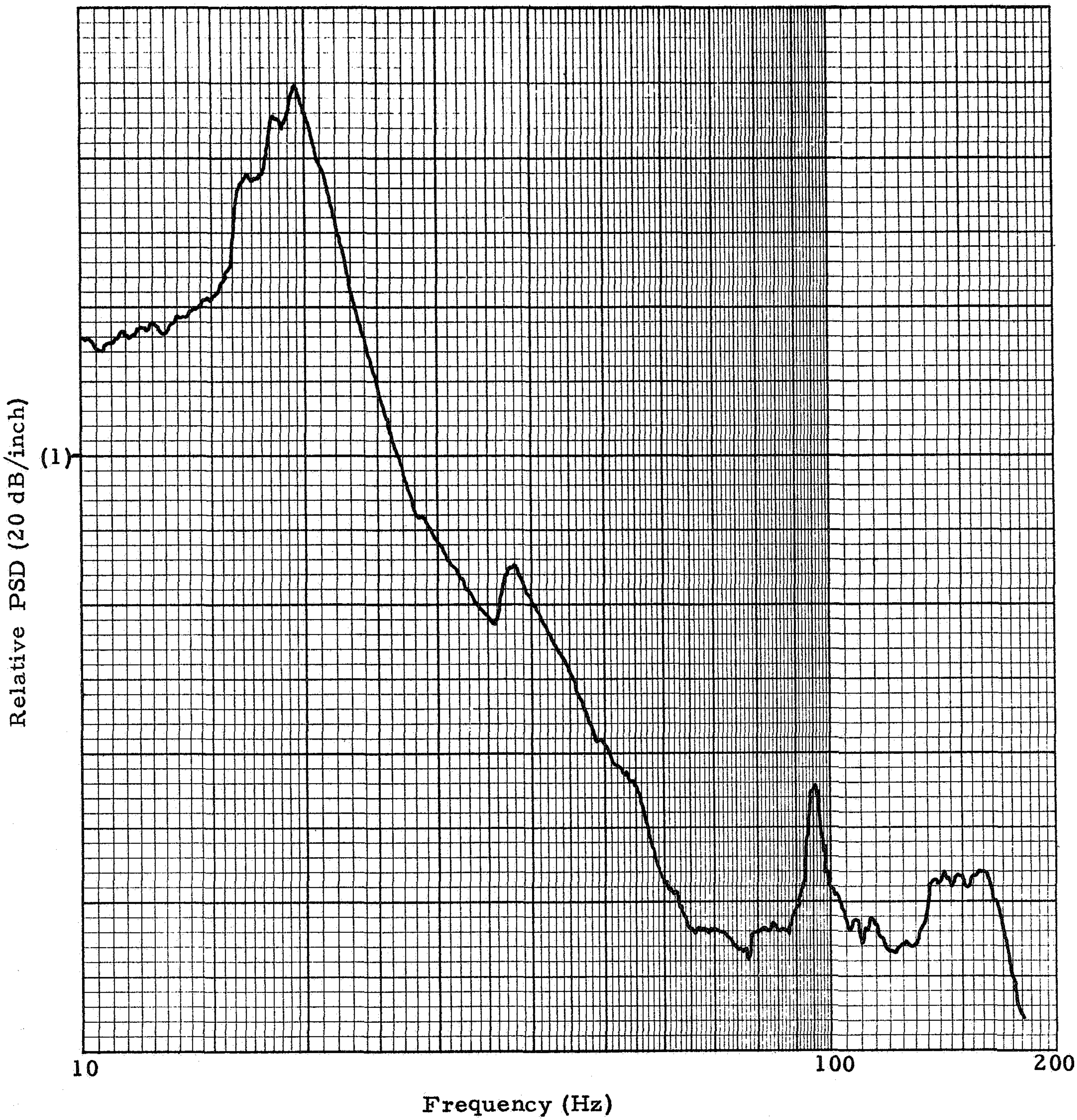

Fig. 5-4 - Sweep Data Point 92-down — Base Bending Moment (1A)

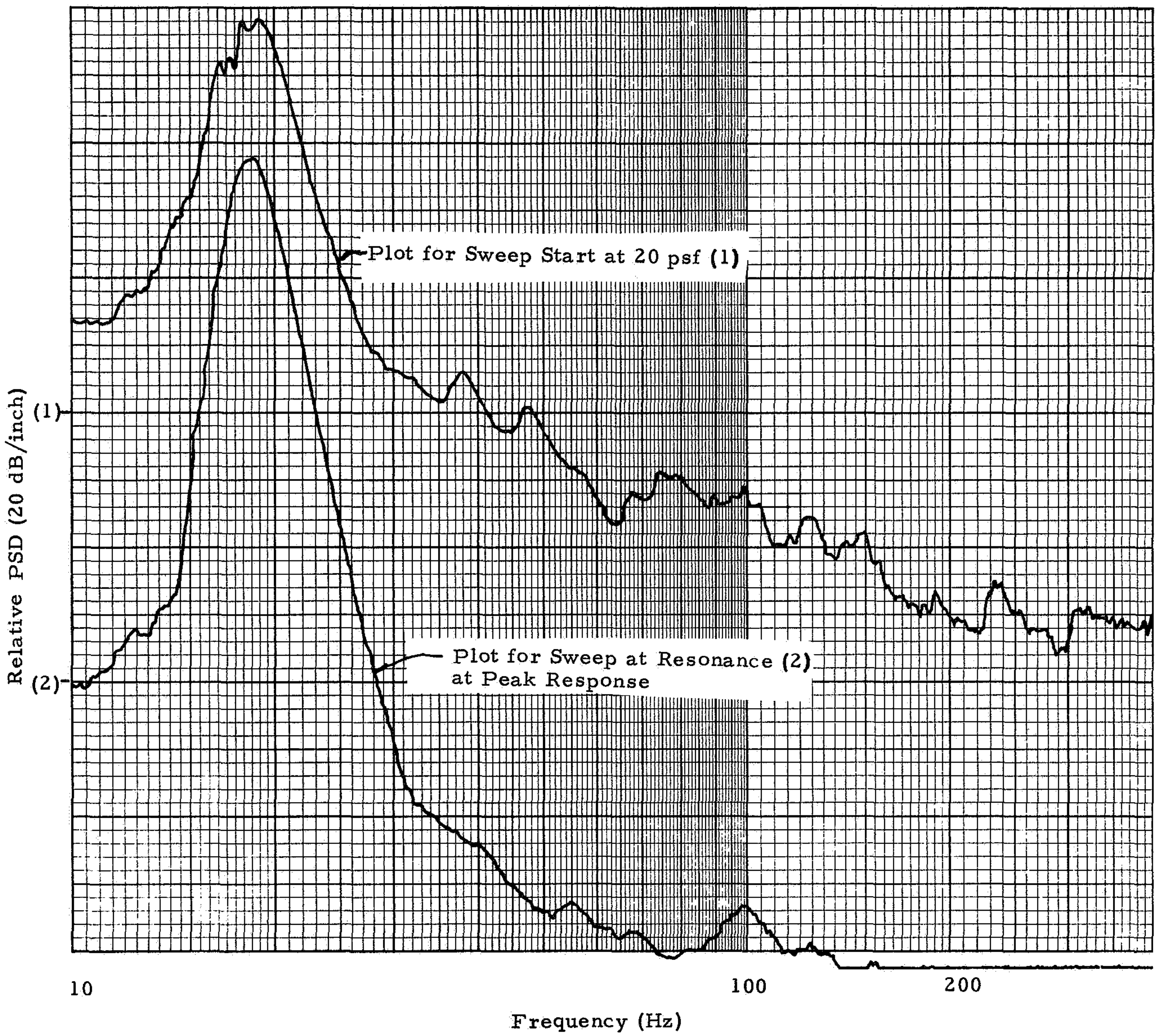

Fig. 5-5 - Sweep Data Point 95 — Base Bending Moment (1A)

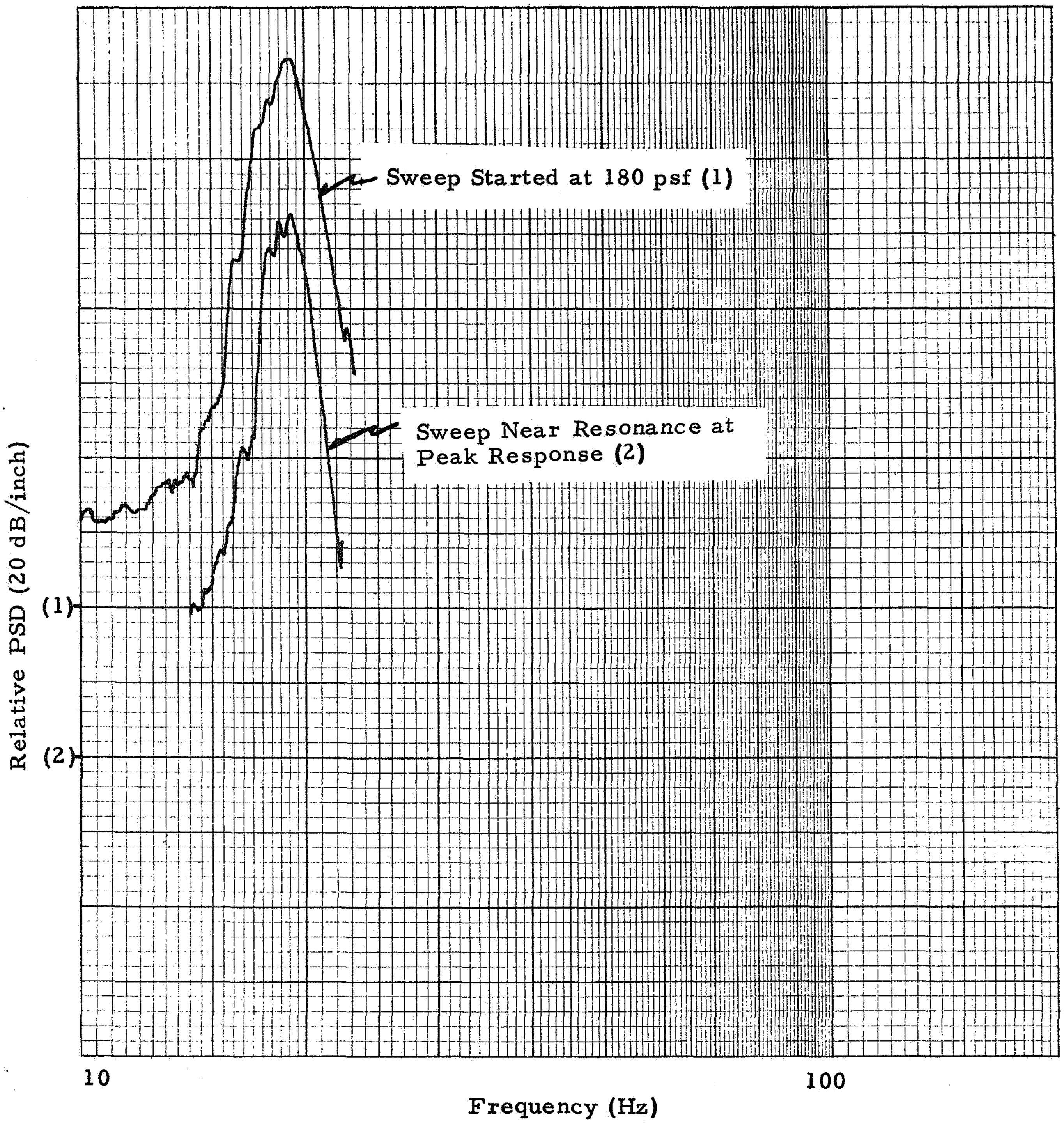

Fig. 5-6 - Sweep Data Point 95-down — Base Bending Moment (1A)

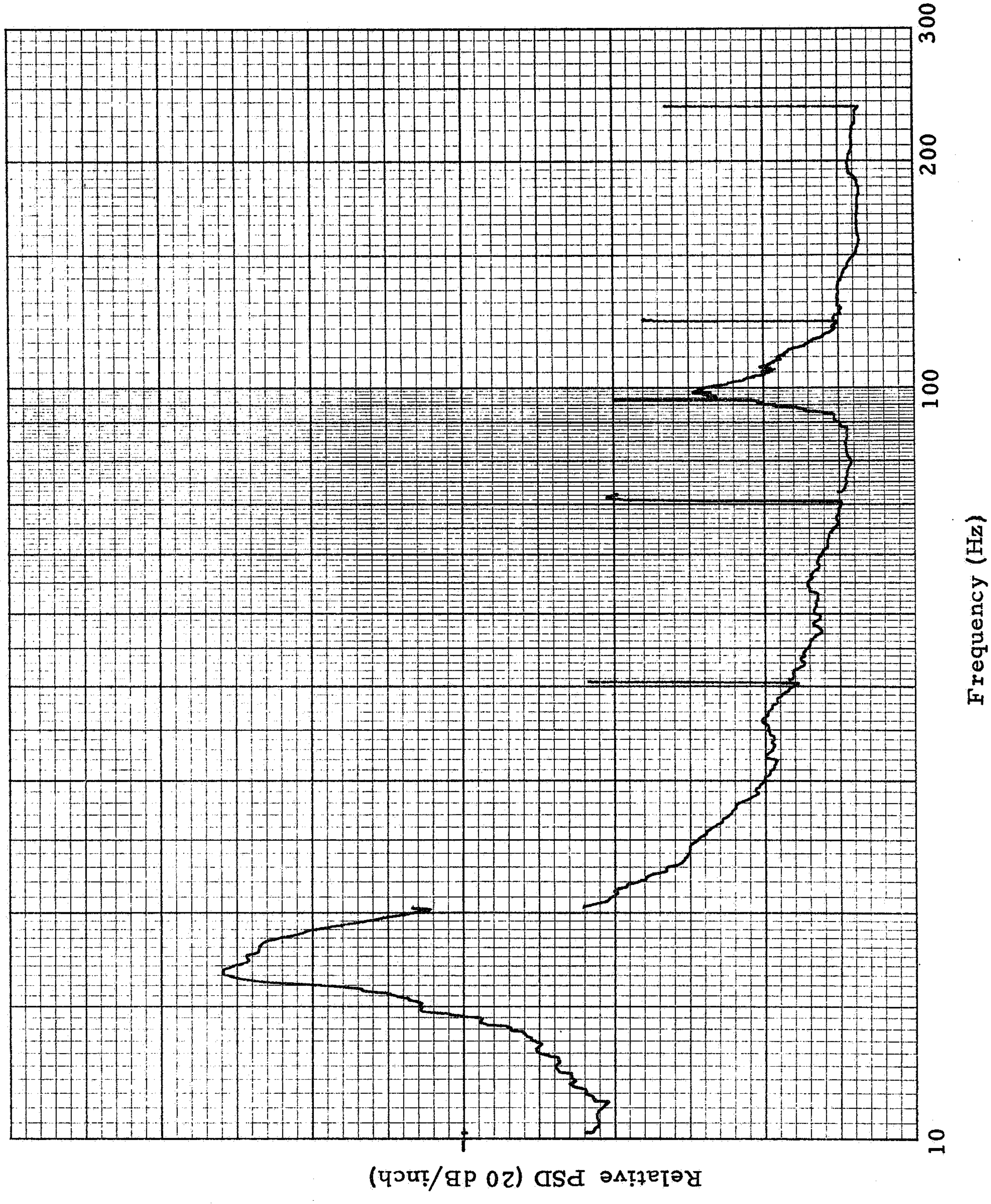

Fig. 5-7 - Dwell Data Point 215 — (2A) Bending Moment

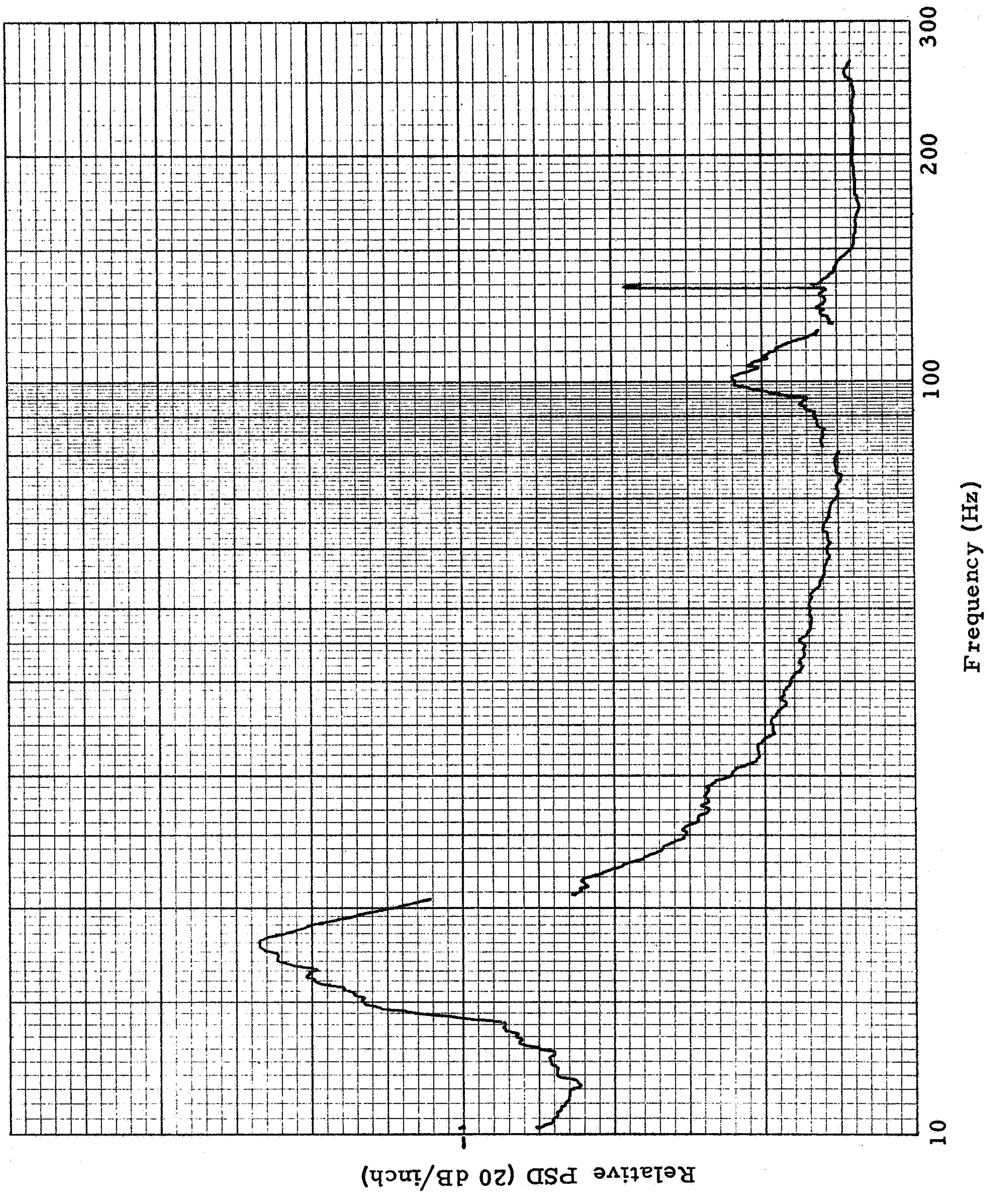

Fig. 5-8 - Dwell Data Point 216 — (2A) Bending Moment

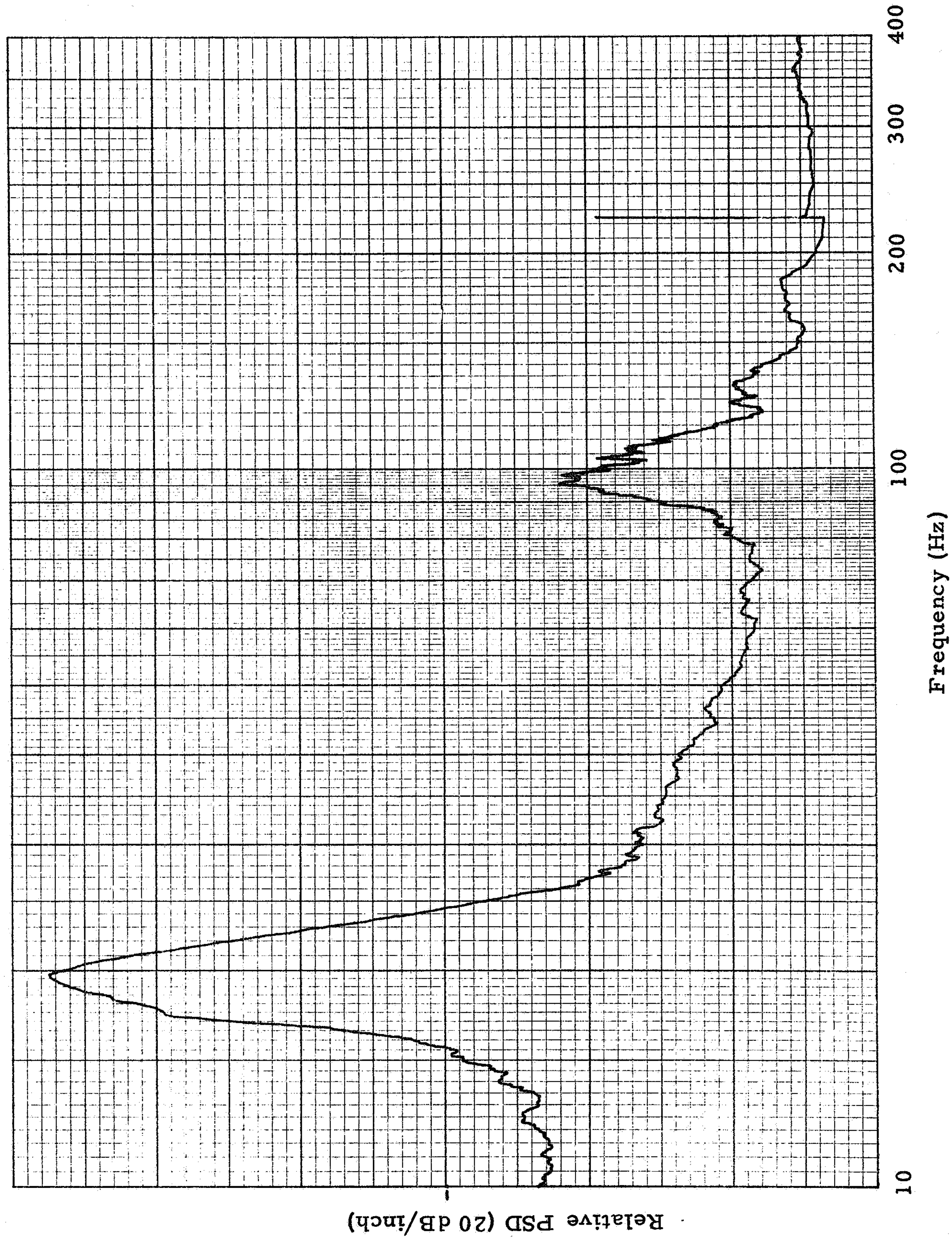

Fig. 5-9 - Sweep Data Point 92 — (2A) Bending Moment

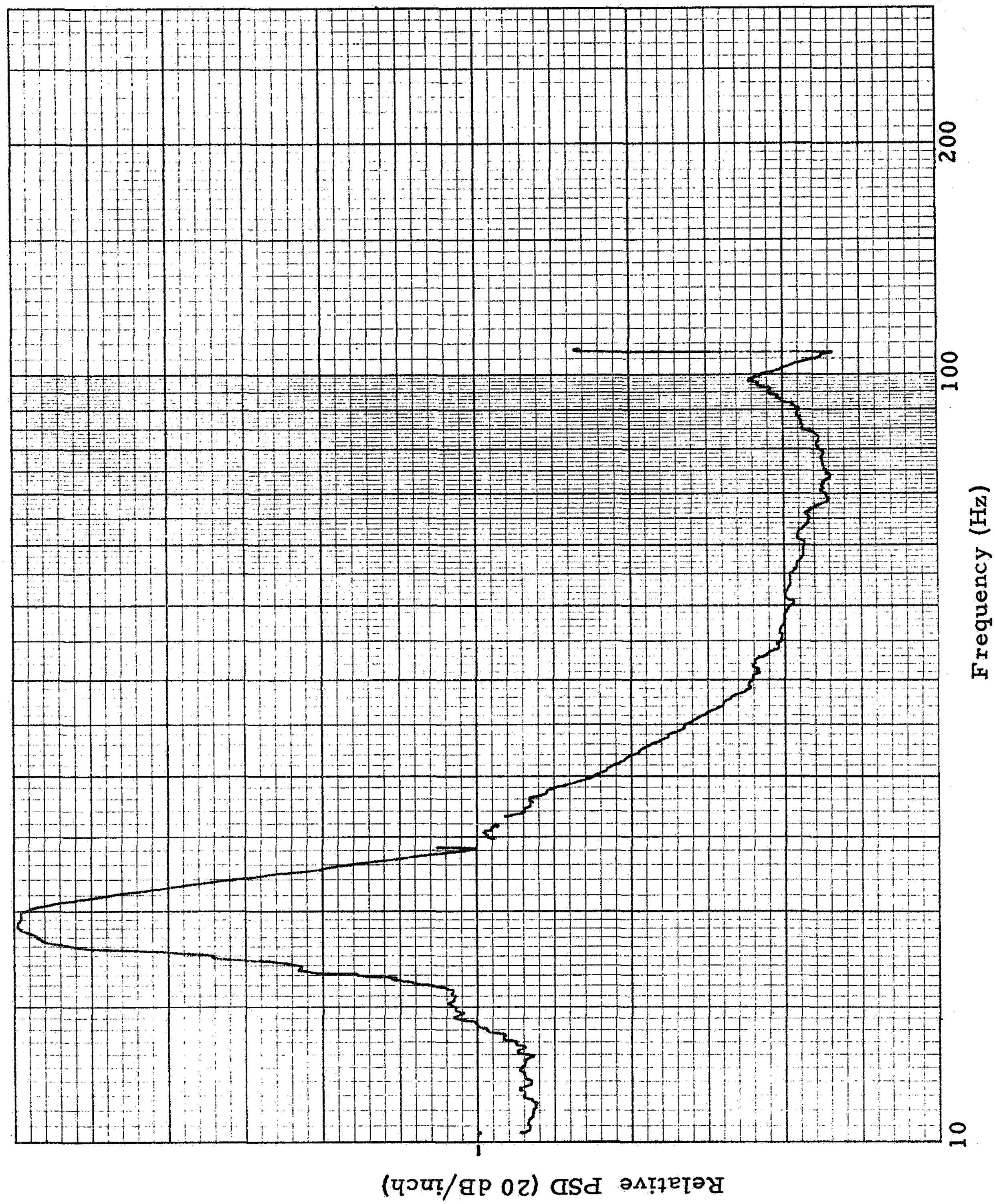

Fig. 5-10 - Sweep Data Point 92-down — (2A) Bending Moment

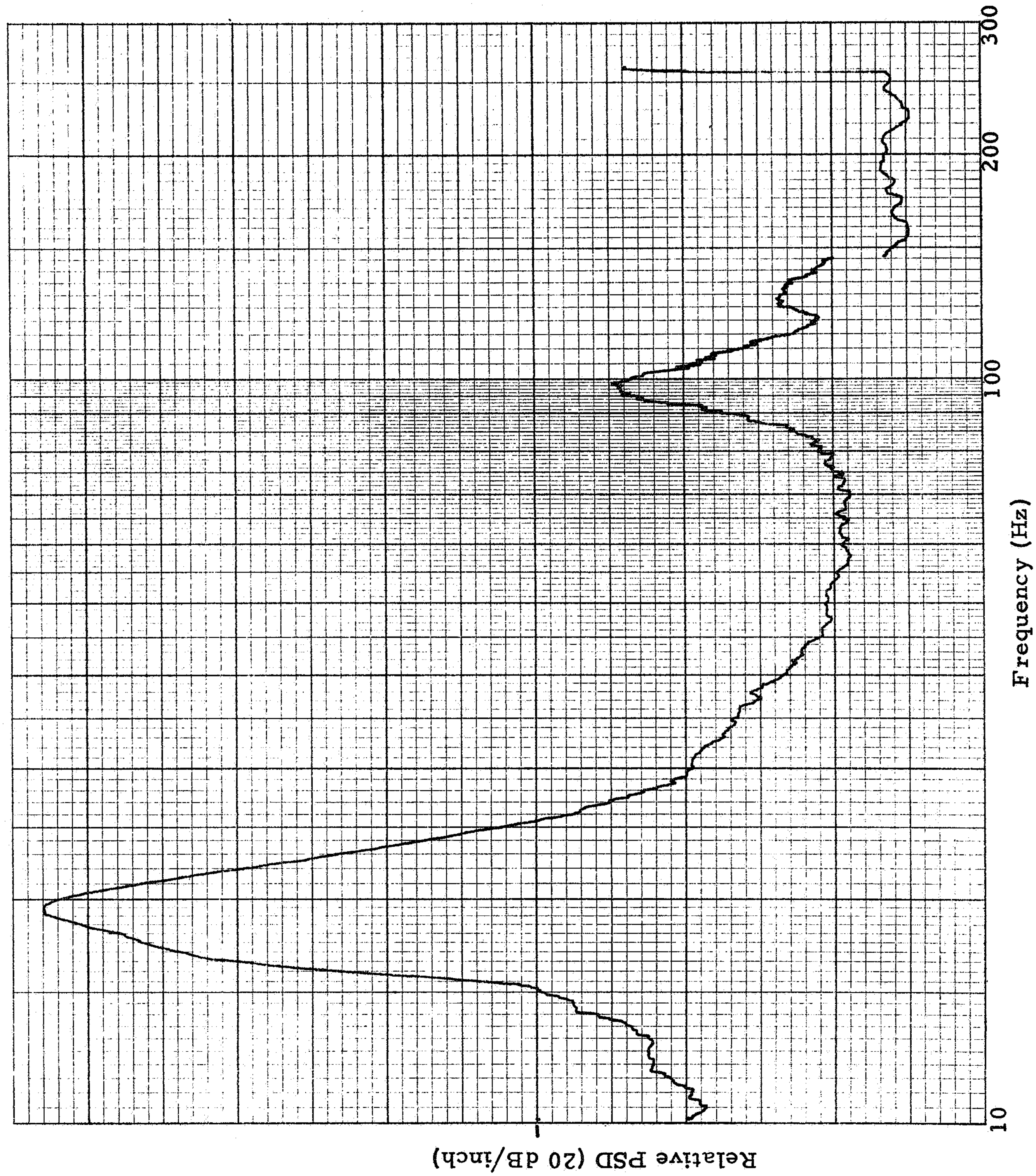

Fig. 5-11 - Sweep Data Point 95 — 2A Bending Moment

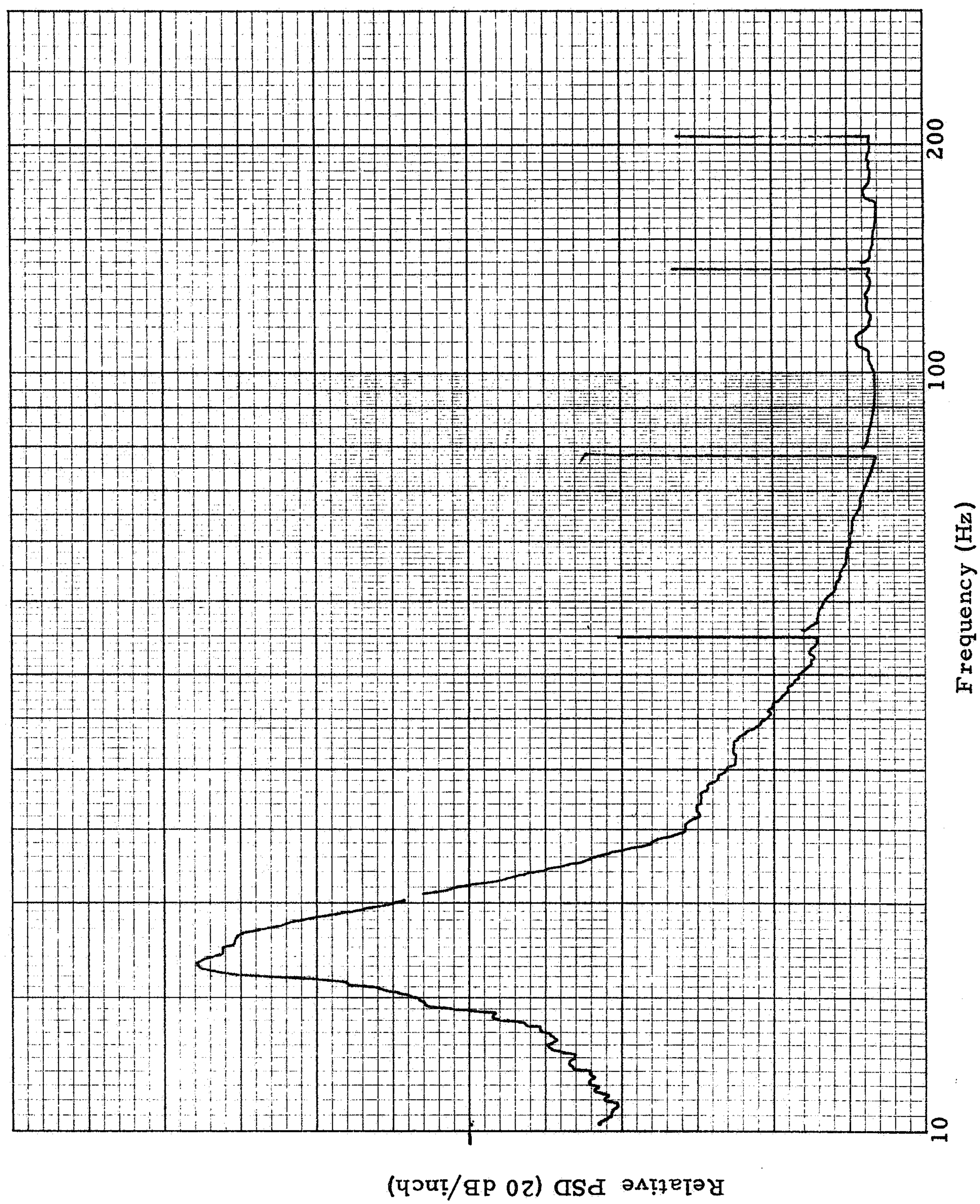

Fig. 5-12 - Dwell Data Point 215 — X-Acceleration (Sta. 90)

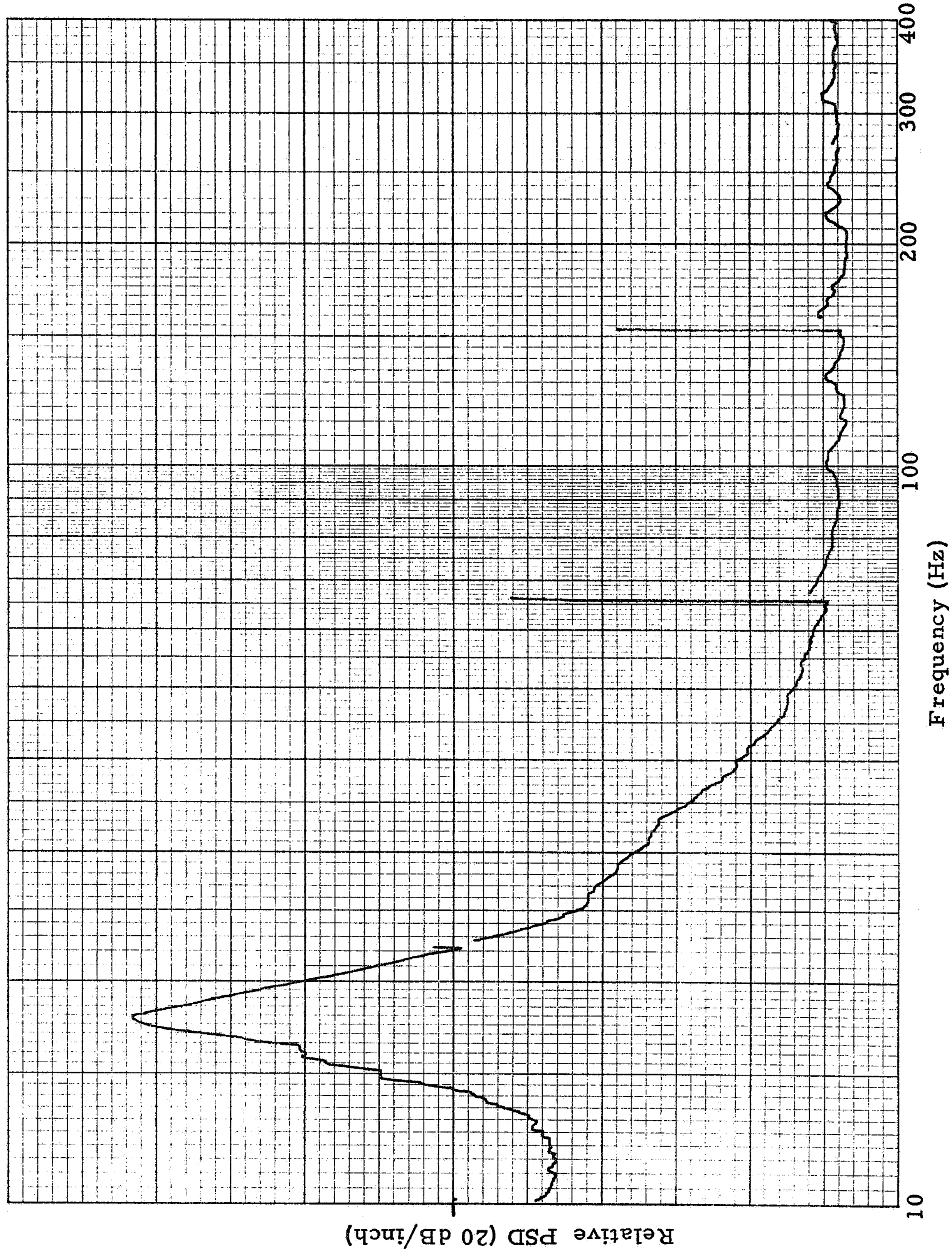

Fig. 5-13 - Dwell Data Point 219 — X Acceleration (Sta. 90)

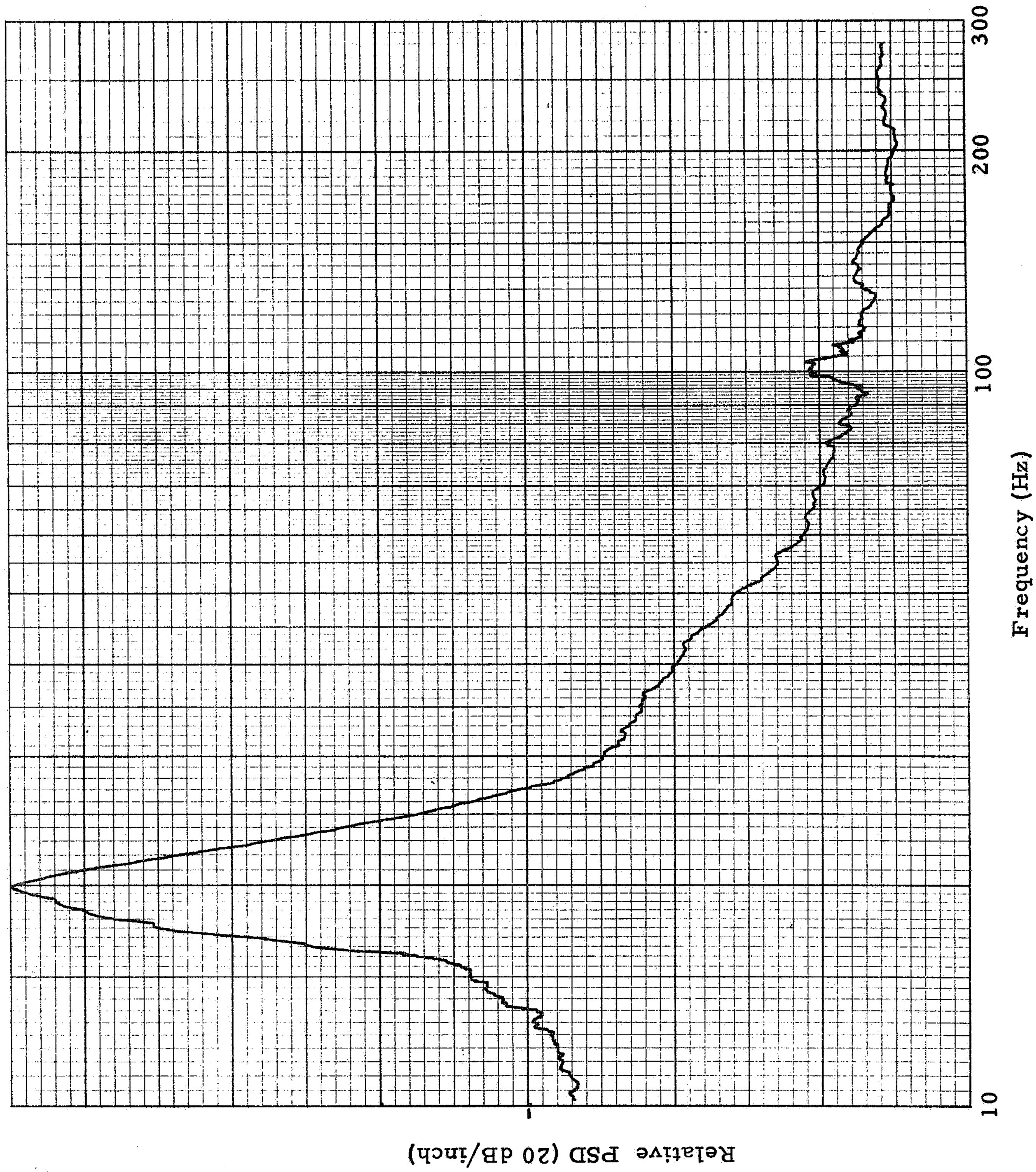

Fig. 5-14 - Sweep Data Point 92 — X-Acceleration (Sta. 90)

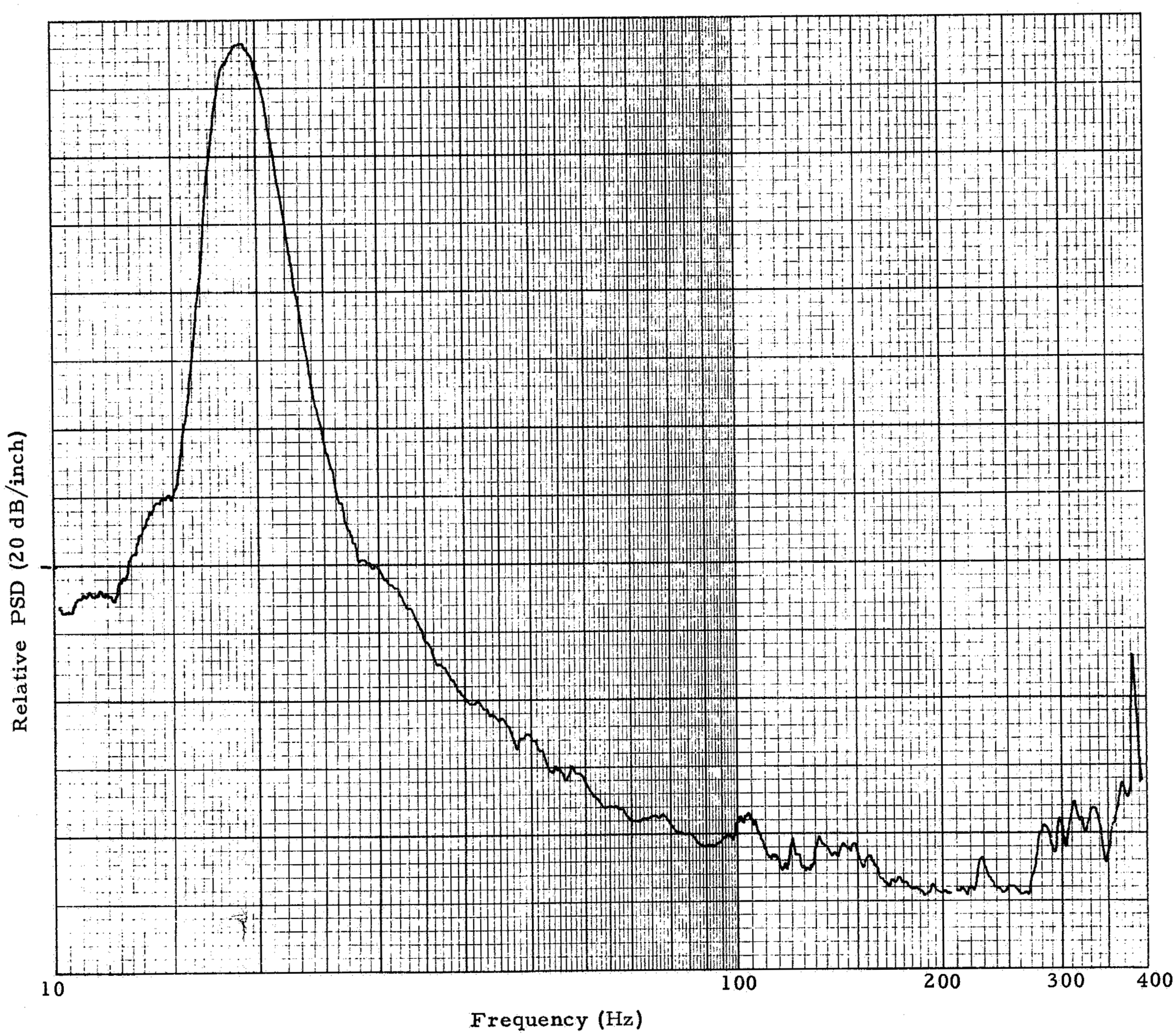

Fig. 5-15 - Sweep Data Point 95 — X-Acceleration (Sta. 90)

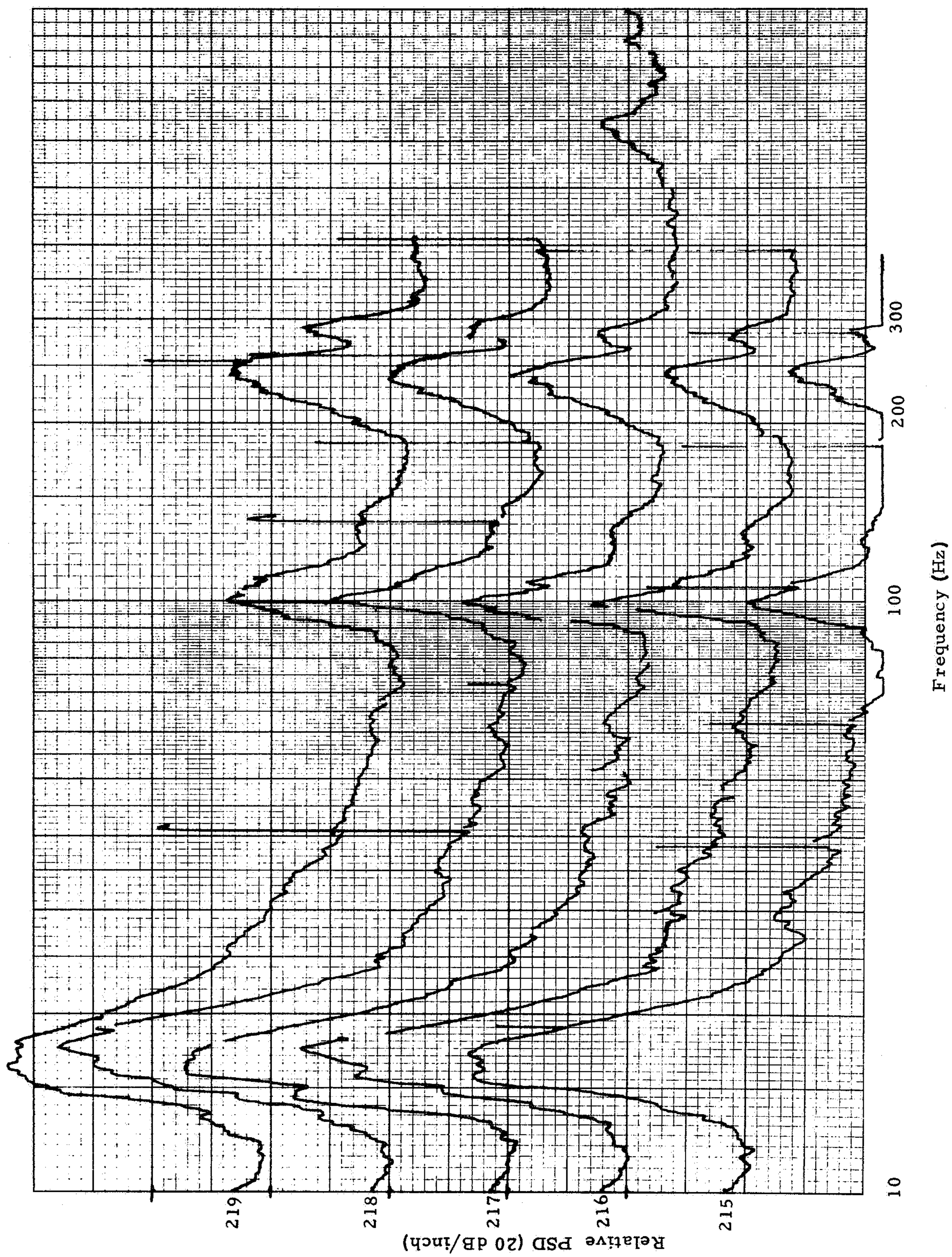

Fig. 5-16 - Dwell Data Points 215 Through 219 — X-Acceleration (Tip)

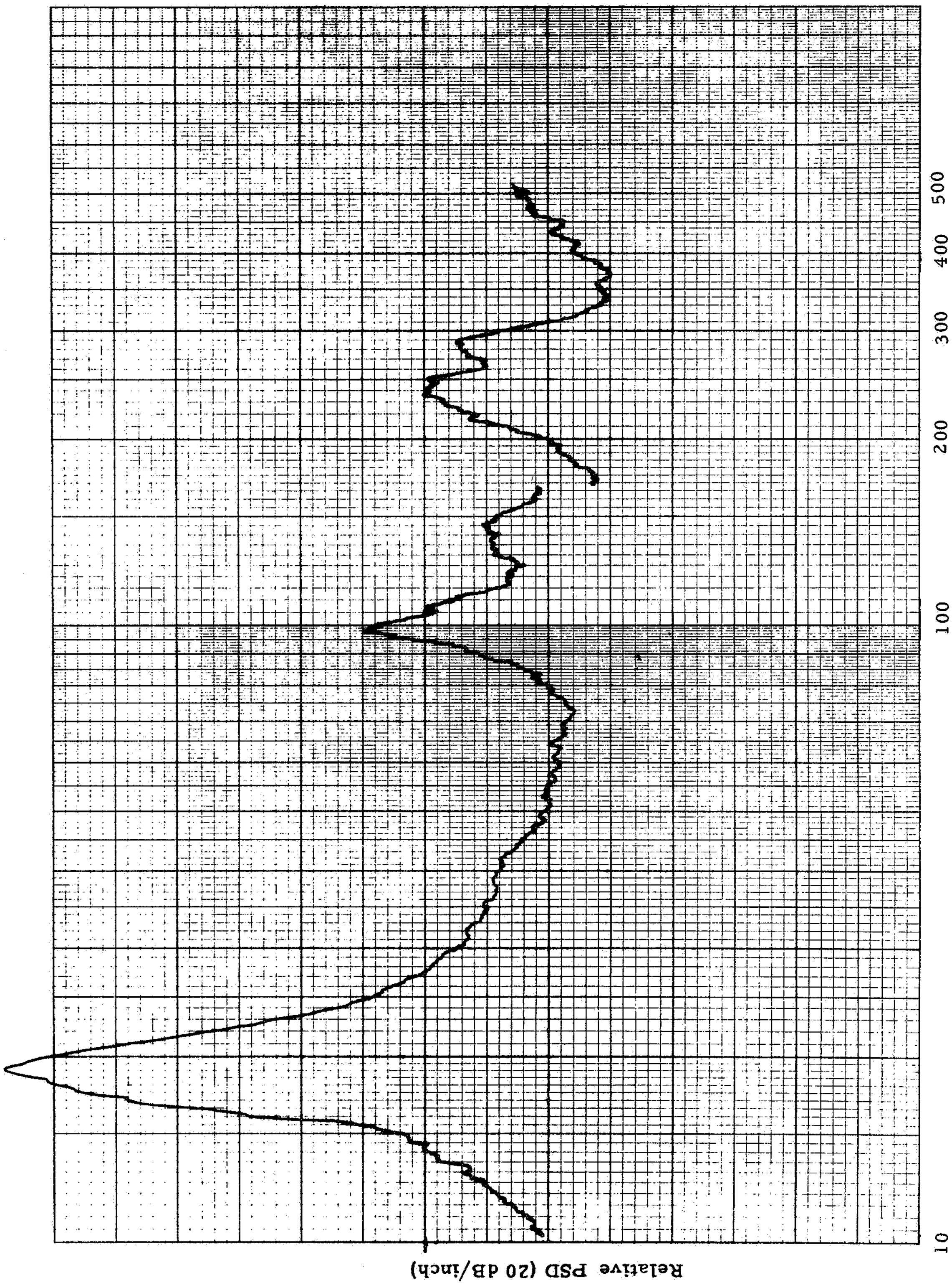

Fig. 5-17 - Sweep Data Point 92 — X-Acceleration (Tip)

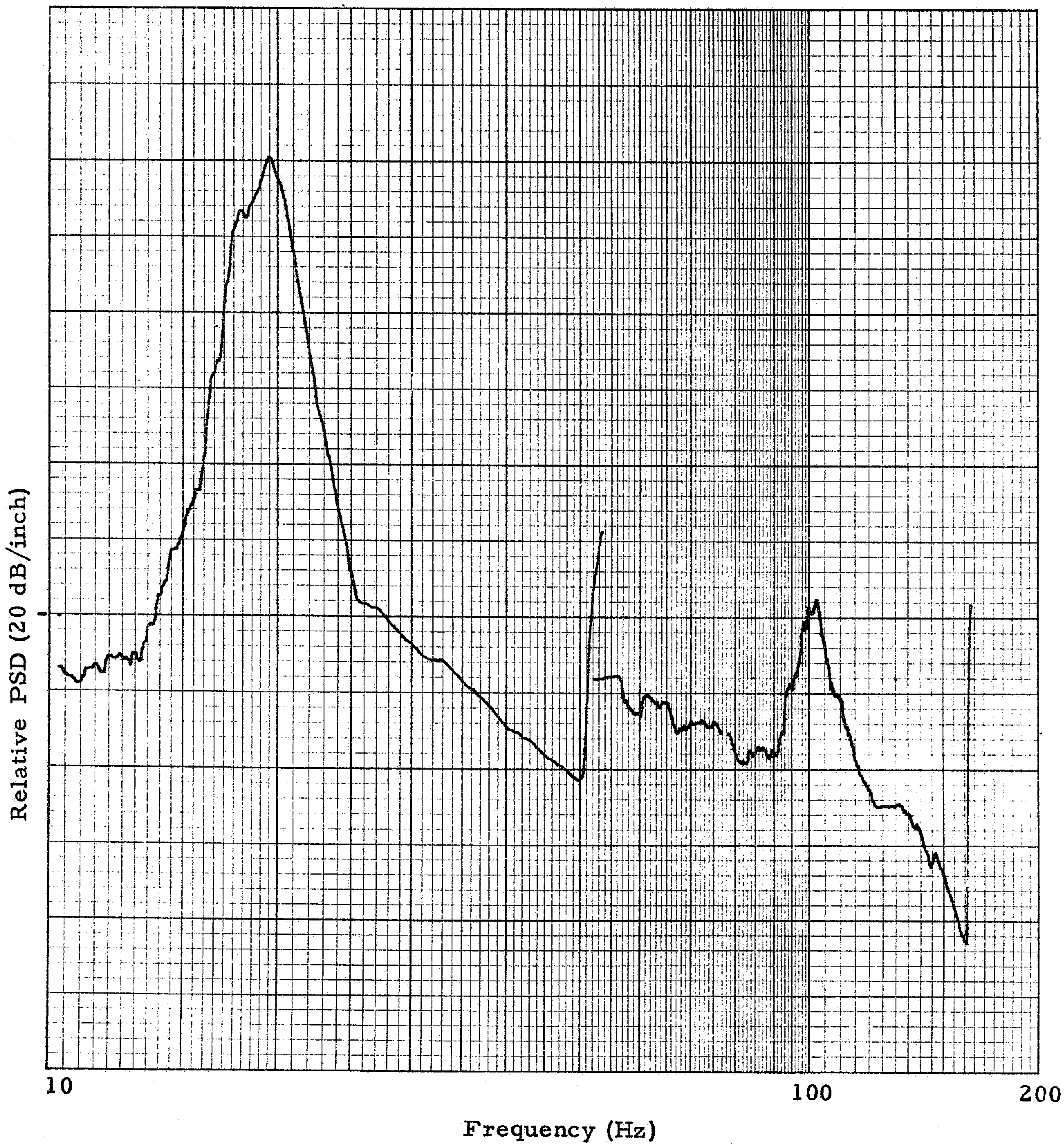

Fig. 5-18 - Sweep Data Point 92-down — X-Acceleration (Tip)

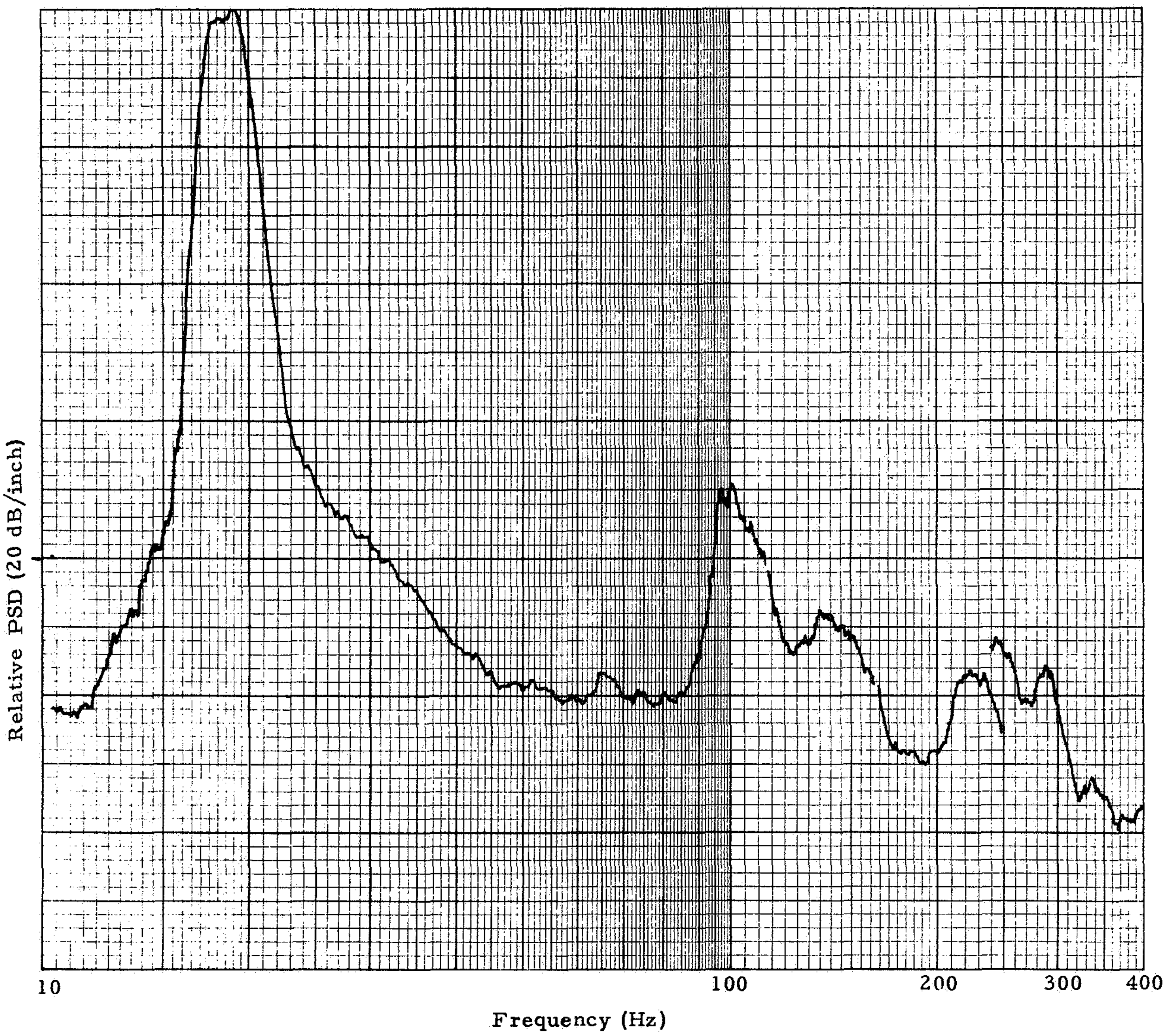

Fig. 5-19 - Sweep Data Point 95 — X Acceleration (Tip)

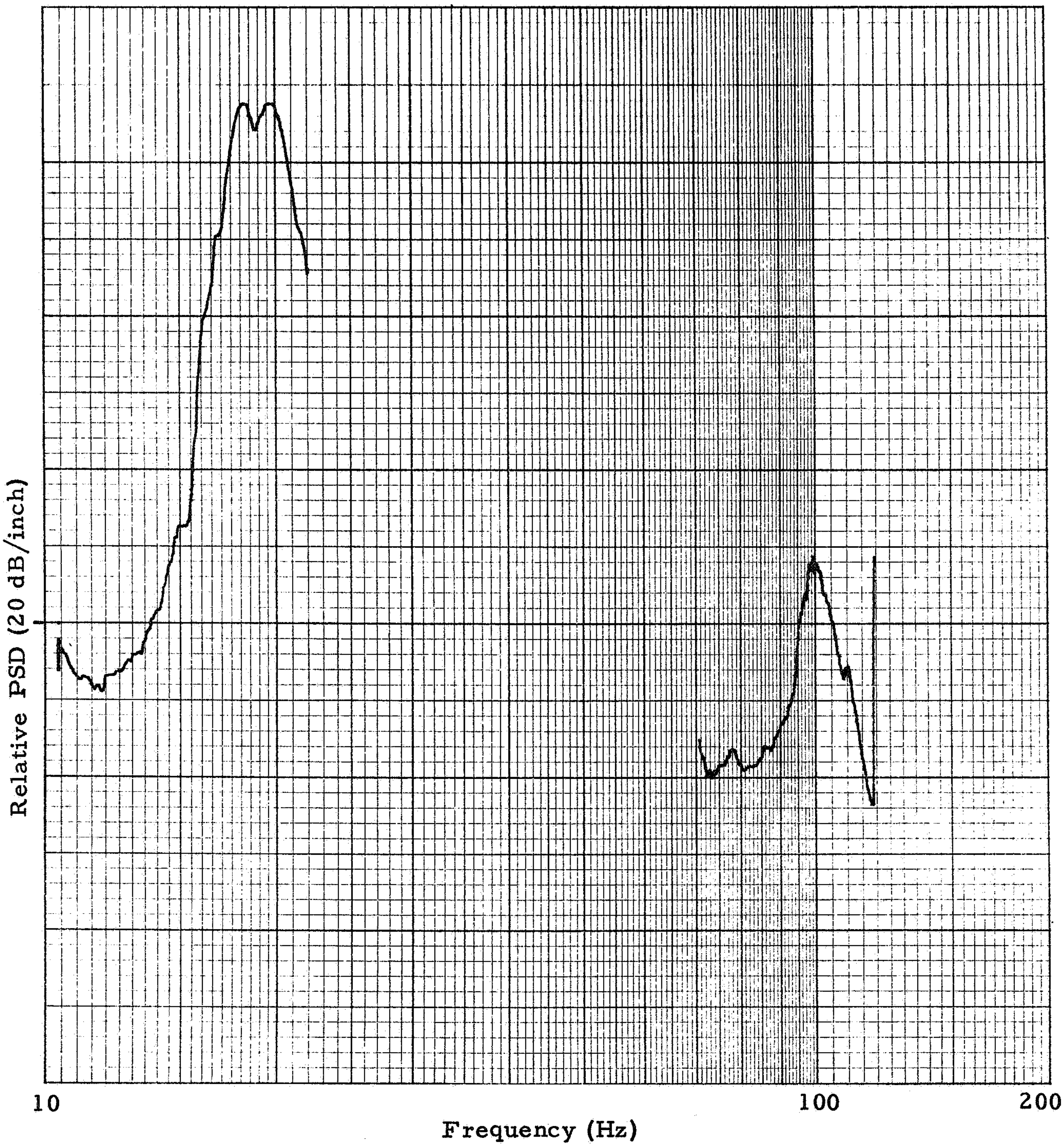

Fig. 5-20 - Sweep Data Point 95-down — X-Acceleration (Tip)

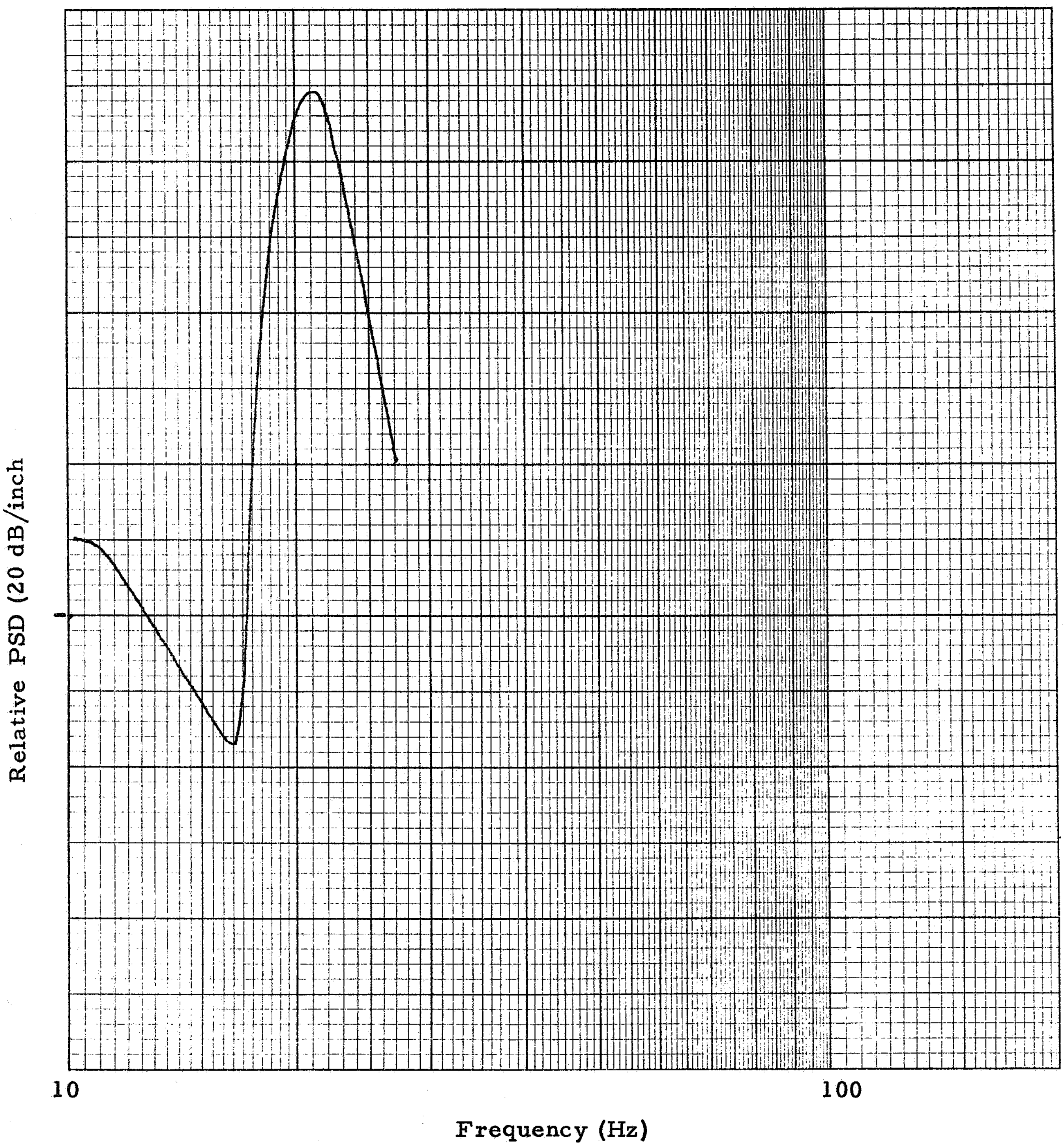

Fig. 5-21 - 20 Hz-Ac Calibrated Signal (Off Tape) Filter Bandwidth = 2 Hz (at 3 dB)

Section 6
CONCLUSIONS AND RECOMMENDATIONS

Testing scaled aeroelastic models in the wind tunnel will continue to be a major part of the design/development of aerospace vehicles. Simulating the characteristics of model structural damping should be considered an important part of the design and planning phase of model development. The level of operational reliability achieved by this model damper system is adequate evidence of its potential application in future ground winds models, such as the Space Shuttle models. A procedure for housing the support post and a method of isolating the torsional and bending elastic modes appear to be the only major design problem areas. Control electronics, circuit design, and feedback sensors are are all proven components in both the current Saturn IB/Skylab program as well as the earlier 3% Saturn V/Dry Workshop Model Test program.

The data analyses presented here are certainly of insufficient scope to draw conclusions on the ground wind response of the total vehicle system. The analyses do show, however, that for the test cases considered, first modal dynamic response is predominant although second- and even third-mode participation is evident. Several basic characteristics of the wind-induced response of elastic bluff bodies remain unsolved. This, in part, is because of the continual necessity for testing, under inherently three-dimensional flow conditions, these "authentic" scale models. Earlier two-dimensional test data have not provided a complete understanding of the phenomenon. Future work in this area is highly recommended.

Other sources of static aerodynamic instability will, of course, appear when bodies with airfoil-like surfaces (i.e., shuttle) are considered. Test programs in which subscale rigid models of the shuttle are used for initial aerodynamic investigation have been proposed. This appears to be a logical first step in the analysis of the complex wind flow about such structures.

Section 7
REFERENCES

1. Scott, L. P., "Saturn IB/Skylab Model Damper Installation and Operation Manual," LMSC-HREC D225270, Lockheed Missiles & Space Company, Huntsville, Ala., August 1971.

2. Lockheed Drawing No. R72107, Revision A, "Damper System for Saturn IB/Skylab 5.5% Model Assembly," 2 March 1971.

3. Keller, A. C., "Considerations in the Analysis of Arbitrary Waveforms," Technical Publication PS-2, Spectral Dynamics Corporation, San Diego, Calif., April 1967.

4. Burrow, L. R., Jr., "Some Analog Methods of Power Spectral Density Analysis," Technical Publication PS-1, Spectral Dynamics Corporation, San Diego, Calif., October 1965.